

Appendix 11. Isotopic Data Results

Contents

Isotopic data results.....	188
Surface waters.....	188
Definition of the Deuterium Excess	188
Groundwater source areas.....	195
Western front.....	195
Shomali subbasin.....	196
Deh Sabz subbasin	196
Eastern front	197
Paghman and upper Kabul subbasin.....	197
Central Kabul	199
Logar subbasin.....	199
Summary observations from stable-isotope data	200
References cited.....	201

Figures

Figure 11-1. Hydrogen isotopic composition, relative to Vienna Standard Mean Ocean Water (VSMOW), of surface water over time in the Kabul Basin, Afghanistan.....	194
Figure 11-2. Oxygen isotopic composition, relative to Vienna Standard Mean Ocean Water (VSMOW), of surface water over time in the Kabul Basin, Afghanistan.....	194
Figure 11-3. The relation between hydrogen and oxygen isotopic composition, relative to Vienna Standard Mean Ocean Water (VSMOW), of all surface waters and of groundwaters and spring in the Western Front Source Area	195
Figure 11-4. The relation between hydrogen and oxygen isotopic composition, relative to Vienna Standard Mean Ocean Water (VSMOW), of all surface waters and of groundwaters and springs in the Shomali subbasin.....	196
Figure 11-5. The relation between hydrogen and oxygen isotopic composition, relative to Vienna Standard Mean Ocean Water (VSMOW), of all surface waters and of groundwaters and springs in the Deh Sabz subbasin	197
Figure 11-6. The relation between hydrogen and oxygen isotopic composition, relative to Vienna Standard Mean Ocean Water (VSMOW), of all surface waters and of groundwaters and springs in the Eastern Front Source Area.....	198
Figure 11-7. The relation between hydrogen and oxygen isotopic composition, relative to Vienna Standard Mean Ocean Water (VSMOW), of all surface waters and of groundwaters and springs in the Paghman and Upper Kabul subbasin.....	198
Figure 11-8. The relation between hydrogen and oxygen isotopic composition, relative to Vienna Standard Mean Ocean Water (VSMOW), of all surface waters and of groundwaters and springs in the Central Kabul subbasin	199
Figure 11-9. The relation between hydrogen and oxygen isotopic composition, relative to Vienna Standard Mean Ocean Water (VSMOW), of all surface waters and of groundwaters and springs in the Logar subbasin	200

Tables

Table 11-1. Stable hydrogen and oxygen isotopic compositions of water analyzed in this study	189
Table 11-2. Mean deuterium excess, d , of selected surface waters	195

Appendix 11. Isotopic Data Results

In this study, 80 groundwater, 4 karez, 7 spring, and 76 surface-water samples were collected and analyzed for determination of $\delta^2\text{H}$ and $\delta^{18}\text{O}$. Between early December 2006 and mid July 2007, surface-water samples were collected at seven sites. The analytical results are shown in table 11-1. Stable hydrogen and oxygen isotopic compositions of these surface waters as a function of time are shown in figures 11-1 and 11-2.

Surface Waters

The measurement data in figures 11-1 and 11-2 show a number of features. Samples from the Istalef River at Istalef and the Paghman River at Paghman surface-water sites are most enriched in ^2H and ^{18}O in accord with the relatively low-elevation source areas in the foothills west of the Kabul Basin. Samples from the Logar River site and Kabul River sites have intermediate $\delta^2\text{H}$ and $\delta^{18}\text{O}$ values reflecting a higher-elevation source area. Between mid-April and June, the $\delta^2\text{H}$ and $\delta^{18}\text{O}$ values of the Logar and Kabul River water increased dramatically, presumably reflecting the sharply decreasing contribution of snowmelt water. The $\delta^2\text{H}$ and $\delta^{18}\text{O}$ values of samples from the Barik Ab River near Bagram were highly variable and may reflect a relatively flashy surface-water system. The lowest $\delta^2\text{H}$ and $\delta^{18}\text{O}$ values were those from the Panjsher River at Sayad and reflect snowmelt water from the high-elevation source area stretching to the Khyber Pass in Pakistan. The lowest $\delta^2\text{H}$ and $\delta^{18}\text{O}$ values in late June presumably reflect the highest fraction of high-elevation snowmelt water.

Definition of the Deuterium Excess

The relation between $\delta^2\text{H}$ and $\delta^{18}\text{O}$ in all water samples analyzed in this study is shown in figure 23. The Global Meteoric Water Line (GMWL) shown is a least squares regression of $\delta^2\text{H}$ and $\delta^{18}\text{O}$ of precipitation at over 200 globally distributed stations (Rozanski and others, 1993) and follows the relation

$$\delta^2\text{H} = 8.20\delta^{18}\text{O} + 11.27 \times 10^3 \quad (11-1)$$

The values of 10^3 are needed to express this relation as a quantity equation rather than as a numeric value equation,

which is desired in the International System of Units (SI). The deuterium excess, d , was defined by Dansgaard (1964) as

$$d = \delta^2\text{H} - 8 \delta^{18}\text{O} \quad (11-2)$$

The value of d is a function of relative humidity (Clark and Fritz, 1997; Merlivat and Jouzel, 1979) with a $10^3 d$ value +20 indicating 70 percent relative humidity and a value of +10 indicating 85 percent relative humidity, which is the global mean. Values of d are shown in table 11-1.

On the basis of d values and $\delta^2\text{H}$ and $\delta^{18}\text{O}$ values (tables 11-1 and 11-2), there appears to be four distinguishable surface-water sources. Samples from the Istalef River at Istalef and the Paghman River at Paghman have overlapping d values and reflect precipitation in the most arid environment (relative humidity is about 70 percent). Samples from the Kabul River at Tang-i-Saidan and the Barik Ab River near Bagram have $10^3 d$ values of about +16.8 and form the second distinguishable source. Samples from the Kabul River at Tang-i-Gharu and the Logar River indicate a third distinguishable source with $10^3 d$ values of about 13.5. The fourth distinguishable source is the Panjsher River at Sayad, which is distinguishable because of its low $\delta^2\text{H}$ and $\delta^{18}\text{O}$ values discussed above. The Barik Ab River near Bagram shows substantial variability in its d value and in its $\delta^2\text{H}$ and $\delta^{18}\text{O}$ values (tables 11-1 and 11-2, figs. 11-1 and 11-2) and may be a small and flashy surface-water source.

There is little evidence of evaporation affecting the isotopic composition of surface waters, which is surprising in this arid environment. The slope of evaporating water on a $\delta^2\text{H}$ versus $\delta^{18}\text{O}$ plot typically is substantially less than 8, and evaporated waters typically plot to the right of the GMWL.

The International Atomic Energy Agency (IAEA) reports $\delta^2\text{H}$ and $\delta^{18}\text{O}$ values for monthly integrated samples of precipitation collected between January 1962 and September 1989 in Kabul (International Atomic Energy Agency/WMO, 2004). The $10^3 \delta^2\text{H}$ values range from -103 to +33 and the $10^3 \delta^{18}\text{O}$ values range from -15.98 to +3.07, and the samples with $10^3 \delta^2\text{H}$ values greater than +15 show substantial evaporation on a $\delta^2\text{H}$ versus $\delta^{18}\text{O}$ plot and were not included in calculations herein. The linear least squares regression of samples having $10^3 \delta^2\text{H}$ values less than +15 is described by

$$10^3 \delta^2\text{H} = 7.73 \times 10^3 \delta^{18}\text{O} + 16.14 \quad (11-3)$$

and is shown in figure 23. This precipitation line is in good agreement with samples from the Istalef River at Istalef and the Paghman River at Paghman.

Table 11-1. Stable hydrogen and oxygen isotopic compositions of water analyzed in this study.

[GW, groundwater; KZ, karez; SP, spring; SW, surface water; VSMOW, Vienna Standard Mean Ocean Water; d, deuterium excess]

Site identification number	Site type	Date	Groundwater area Surface-water site	$10^3 \delta^2\text{H}$ relative to VSMOW	$10^3 \delta^{18}\text{O}$ relative to VSMOW	$10^3 d$
64	GW	06-24-2006	Central Kabul	-55.9	-8.87	15.06
65	GW	05-25-2006	Central Kabul	-60.7	-9.28	13.54
124	GW	05-27-2006	Central Kabul	-56.1	-8.87	14.86
129	GW	05-24-2006	Central Kabul	-55.6	-8.79	14.72
133	GW	05-27-2006	Central Kabul	-55.0	-8.52	13.16
148	GW	06-05-2006	Central Kabul	-55.3	-7.97	8.46
152	GW	06-05-2006	Central Kabul	-52.5	-8.24	13.42
153	GW	05-20-2006	Central Kabul	-45.4	-7.34	13.32
156	GW	05-27-2006	Central Kabul	-46.1	-7.18	11.34
157	GW	05-27-2006	Central Kabul	-57.6	-8.56	10.88
162.2	GW	05-31-2006	Central Kabul	-55.2	-8.58	13.44
163	GW	05-31-2006	Central Kabul	-53.3	-8.38	13.74
165	GW	05-22-2006	Central Kabul	-59.0	-9.14	14.12
167	GW	06-20-2006	Central Kabul	-62.4	-9.37	12.56
168	GW	05-22-2006	Central Kabul	-58.0	-9.06	14.48
170	GW	06-18-2006	Central Kabul	-50.3	-7.75	11.7
172	GW	05-22-2006	Central Kabul	-54.6	-8.50	13.4
173	GW	06-18-2006	Central Kabul	-60.3	-9.17	13.06
183	GW	06-04-2007	Central Kabul	-54.2	-8.62	14.76
185	GW	06-16-2007	Central Kabul	-58.6	-8.97	13.16
186	GW	06-18-2007	Central Kabul	-62.4	-9.36	12.48
208	GW	05-20-2006	Central Kabul	-56.2	-8.89	14.92
210	GW	05-31-2006	Central Kabul	-55.1	-8.76	14.98
218	GW	06-20-2006	Central Kabul	-64.5	-9.56	11.98
219	GW	06-20-2006	Central Kabul	-63.3	-9.38	11.74
220	GW	06-20-2006	Central Kabul	-61.9	-9.29	12.42
223	GW	02-22-2007	Central Kabul	-59.1	-9.16	14.18
8	GW	06-07-2006	Deh Sabz	-55.0	-8.29	11.32
13	GW	05-16-2006	Deh Sabz	-56.6	-8.98	15.24
15	GW	05-30-2006	Deh Sabz	-52.4	-8.02	11.76
37	GW	05-14-2006	Deh Sabz	-63.0	-9.69	14.52
54	GW	05-21-2006	Deh Sabz	-59.1	-9.03	13.14
2.1	GW	06-07-2006	Eastern Front	-58.9	-9.70	18.7
7	GW	06-04-2006	Eastern Front	-48.8	-8.78	21.44
59.1	GW	05-10-2006	Eastern Front	-55.2	-9.30	19.2
71	GW	06-05-2007	Eastern Front	-56.5	-9.46	19.18
116	GW	05-29-2006	Logar	-54.7	-8.58	13.94
135	GW	05-17-2006	Logar	-53.9	-8.28	12.34

Table 11-1. Stable hydrogen and oxygen isotopic compositions of water analyzed in this study.—Continued

[GW, groundwater; KZ, karez; SP, spring; SW, surface water; VSMOW, Vienna Standard Mean Ocean Water; d, deuterium excess]

Site identification number	Site type	Date	Groundwater area Surface-water site	$10^3 \delta^2\text{H}$ relative to VSMOW	$10^3 \delta^{18}\text{O}$ relative to VSMOW	$10^3 d$
140	GW	05-29-2006	Logar	-54.7	-8.18	10.74
143	GW	05-29-2006	Logar	-55.3	-8.27	10.86
187	GW	06-20-2007	Logar	-54.6	-8.25	11.4
201	GW	06-13-2006	Logar	-56.2	-8.41	11.08
202	GW	06-13-2006	Logar	-56.8	-8.45	10.8
203	GW	05-20-2006	Logar	-56.8	-8.60	12
204	GW	06-13-2006	Logar	-56.4	-8.33	10.24
221	GW	12-05-2006	Logar	-56.1	-8.44	11.42
107	GW	05-15-2006	Paghman and Upper Kabul	-59.8	-9.29	14.52
112	GW	06-03-2006	Paghman and Upper Kabul	-55.3	-8.47	12.46
113	GW	05-29-2006	Paghman and Upper Kabul	-56.2	-8.84	14.52
115	GW	05-29-2006	Paghman and Upper Kabul	-47.5	-8.43	19.94
117	GW	05-15-2006	Paghman and Upper Kabul	-53.1	-8.48	14.74
182	GW	06-02-2007	Paghman and Upper Kabul	-50.5	-8.48	17.34
184	GW	06-06-2007	Paghman and Upper Kabul	-56.6	-8.96	15.08
211	GW	06-08-2006	Paghman and Upper Kabul	-56.2	-8.76	13.88
212	GW	06-08-2006	Paghman and Upper Kabul	-55.0	-8.78	15.24
213	GW	05-15-2006	Paghman and Upper Kabul	-54.3	-8.74	15.62
214	GW	06-11-2006	Paghman and Upper Kabul	-50.6	-8.04	13.72
216	GW	06-11-2006	Paghman and Upper Kabul	-53.5	-8.60	15.3
217	GW	06-11-2006	Paghman and Upper Kabul	-52.4	-8.43	15.04
222	GW	12-10-2006	Paghman and Upper Kabul	-56.2	-9.04	16.12
22.1	GW	06-12-2006	Shomali	-47.9	-8.11	16.98
24	GW	06-14-2006	Shomali	-50.1	-8.47	17.66
25	GW	06-14-2006	Shomali	-52.8	-8.55	15.6
28	GW	05-23-2006	Shomali	-52.4	-8.49	15.52
42	GW	05-28-2006	Shomali	-55.8	-9.08	16.84
47	GW	05-30-2006	Shomali	-53.7	-8.62	15.26
72	GW	06-12-2007	Shomali	-50.0	-8.39	17.12
74	GW	06-19-2007	Shomali	-57.5	-9.17	15.86
20	GW	06-10-2006	Western Front	-45.8	-8.16	19.48
21	GW	06-12-2006	Western Front	-53.1	-9.01	18.98
33	GW	05-23-2006	Western Front	-49.5	-8.43	17.94
41	GW	05-28-2006	Western Front	-50.2	-8.70	19.4
43	GW	05-28-2006	Western Front	-52.3	-8.90	18.9
45	GW	05-30-2006	Western Front	-56.2	-9.29	18.12
52	GW	06-10-2006	Western Front	-45.7	-8.15	19.5

Table 11-1. Stable hydrogen and oxygen isotopic compositions of water analyzed in this study.—Continued

[GW, groundwater; KZ, karez; SP, spring; SW, surface water; VSMOW, Vienna Standard Mean Ocean Water; d, deuterium excess]

Site identification number	Site type	Date	Groundwater area Surface-water site	10 ³ δ ² H relative to VSMOW	10 ³ δ ¹⁸ O relative to VSMOW	10 ³ d
67	GW	12-09-2006	Western Front	-56.9	-9.34	17.82
100	GW	06-03-2006	Western Front	-46.8	-8.19	18.72
104	GW	05-13-2006	Paghman and Upper Kabul	-50.3	-8.46	17.38
104	GW	12-03-2006	Paghman and Upper Kabul	-48.3	-8.34	18.42
73	GW	06-17-2007	Western Front	-55.0	-9.18	18.44
6	KZ	05-10-2006	Eastern Front	-54.0	-9.04	18.32
10	KZ	05-10-2006	Eastern Front	-54.6	-9.23	19.24
69.1	KZ	05-10-2006	Eastern Front	-50.0	-8.72	19.76
105	KZ	05-13-2006	Paghman and Upper Kabul	-41.9	-6.94	13.62
180	SP	05-17-2006	Central Kabul	-53.5	-8.60	15.3
66.1	SP	05-10-2006	Eastern Front	-50.5	-8.85	20.3
181	SP	05-17-2006	Logar	-55.1	-8.79	15.22
67.1	SP	05-23-2006	Shomali	-49.9	-8.24	16.02
68.1	SP	05-21-2006	Shomali	-50.1	-8.38	16.94
101	SP	05-13-2006	Western Front	-45.9	-8.16	19.38
67.2	SP	06-17-2006	Western Front	-51.7	-8.53	16.54
301	SW	12-04-2006	Istalef River	-54.8	-9.44	20.72
301	SW	12-18-2006	Istalef River	-47.7	-8.38	19.34
301	SW	01-02-2007	Istalef River	-48.4	-8.42	18.96
301	SW	01-16-2007	Istalef River	-47.6	-8.49	20.32
301	SW	01-30-2007	Istalef River	-47.7	-8.39	19.42
301	SW	02-13-2007	Istalef River	-50.7	-8.75	19.3
301	SW	02-27-2007	Istalef River	-52.3	-8.75	17.7
301	SW	03-13-2007	Istalef River	-52.0	-8.90	19.2
301	SW	03-27-2007	Istalef River	-52.9	-9.12	20.06
301	SW	04-10-2007	Istalef River	-51.6	-9.09	21.12
301	SW	04-24-2007	Istalef River	-52.9	-9.16	20.38
301	SW	06-14-2007	Istalef River	-52.4	-9.06	20.08
301	SW	07-15-2007	Istalef River	-48.8	-8.52	19.36
302	SW	12-09-2006	Panjsher River at Sayad	-61.9	-10.02	18.26

Table 11-1. Stable hydrogen and oxygen isotopic compositions of water analyzed in this study.—Continued

[GW, groundwater; KZ, karez; SP, spring; SW, surface water; VSMOW, Vienna Standard Mean Ocean Water; d, deuterium excess]

Site identification number	Site type	Date	Groundwater area Surface-water site	$10^3 \delta^2\text{H}$ relative to VSMOW	$10^3 \delta^{18}\text{O}$ relative to VSMOW	$10^3 d$
302	SW	12-26-2006	Panjsher River at Sayad	-60.1	-9.79	18.22
302	SW	01-09-2007	Panjsher River at Sayad	-61.6	-9.92	17.76
302	SW	01-23-2007	Panjsher River at Sayad	-62.4	-9.90	16.8
302	SW	02-06-2007	Panjsher River at Sayad	-60.9	-9.81	17.58
302	SW	02-20-2007	Panjsher River at Sayad	-60.7	-9.84	18.02
302	SW	03-06-2007	Panjsher River at Sayad	-59.1	-9.74	18.82
302	SW	03-20-2007	Panjsher River at Sayad	-63.4	-10.25	18.6
302	SW	04-03-2007	Panjsher River at Sayad	-62.1	-9.95	17.5
302	SW	04-17-2007	Panjsher River at Sayad	-59.7	-9.83	18.94
302	SW	06-19-2007	Panjsher River at Sayad	-66.5	-10.68	18.94
303	SW	12-26-2006	Barik Ab River	-63.1	-9.91	16.18
303	SW	01-09-2007	Barik Ab River	-62.9	-9.73	14.94
303	SW	01-23-2007	Barik Ab River	-62.4	-9.70	15.2
303	SW	02-20-2007	Barik Ab River	-53.3	-8.51	14.78
303	SW	03-06-2007	Barik Ab River	-60.2	-9.47	15.56
303	SW	03-20-2007	Barik Ab River	-50.5	-8.52	17.66
303	SW	04-03-2007	Barik Ab River	-51.3	-8.84	19.42
303	SW	04-17-2007	Barik Ab River	-55.4	-9.48	20.44
321	SW	12-05-2006	Logar River	-61.0	-9.44	14.52
321	SW	12-19-2006	Logar River	-61.6	-9.28	12.64
321	SW	01-06-2007	Logar River	-61.1	-9.28	13.14
321	SW	01-21-2007	Logar River	-61.5	-9.24	12.42
321	SW	02-07-2007	Logar River	-61.2	-9.41	14.08
321	SW	02-21-2007	Logar River	-60.4	-9.25	13.6
321	SW	03-07-2007	Logar River	-60.2	-9.02	11.96
321	SW	03-19-2007	Logar River	-58.6	-9.14	14.52
321	SW	04-04-2007	Logar River	-60.2	-9.22	13.56
321	SW	04-18-2007	Logar River	-59.5	-9.27	14.66
321	SW	06-20-2007	Logar River	-51.7	-7.65	9.5
322	SW	12-05-2006	Kabul River at Tang-i-Gharu	-58.0	-8.95	13.6
322	SW	12-25-2006	Kabul River at Tang-i-Gharu	-60.0	-9.23	13.84
322	SW	01-06-2007	Kabul River at Tang-i-Gharu	-59.9	-9.12	13.06
322	SW	01-21-2007	Kabul River at Tang-i-Gharu	-58.4	-9.04	13.92
322	SW	02-07-2007	Kabul River at Tang-i-Gharu	-59.6	-9.11	13.28
322	SW	02-21-2007	Kabul River at Tang-i-Gharu	-60.7	-9.24	13.22
322	SW	03-07-2007	Kabul River at Tang-i-Gharu	-57.7	-8.93	13.74
322	SW	03-19-2007	Kabul River at Tang-i-Gharu	-55.0	-8.80	15.4

Table 11-1. Stable hydrogen and oxygen isotopic compositions of water analyzed in this study.—Continued

[GW, groundwater; KZ, karez; SP, spring; SW, surface water; VSMOW, Vienna Standard Mean Ocean Water; d, deuterium excess]

Site identification number	Site type	Date	Groundwater area Surface-water site	$10^3 \delta^2\text{H}$ relative to VSMOW	$10^3 \delta^{18}\text{O}$ relative to VSMOW	$10^3 d$
322	SW	04-18-2007	Kabul River at Tang-i-Gharu	-59.3	-9.48	16.54
322	SW	06-04-2007	Kabul River at Tang-i-Gharu	-47.7	-7.71	13.98
322	SW	07-04-2007	Kabul River at Tang-i-Gharu	-54.1	-8.27	12.06
323	SW	12-10-2006	Paghman River at Pul-i-Sokhta	-47.2	-8.62	21.76
323	SW	12-25-2006	Paghman River at Pul-i-Sokhta	-49.8	-8.70	19.8
323	SW	01-10-2007	Paghman River at Pul-i-Sokhta	-49.2	-8.58	19.44
323	SW	01-25-2007	Paghman River at Pul-i-Sokhta	-48.0	-8.60	20.8
323	SW	02-10-2007	Paghman River at Pul-i-Sokhta	-52.9	-9.22	20.86
323	SW	02-24-2007	Paghman River at Pul-i-Sokhta	-52.9	-9.04	19.42
323	SW	03-10-2007	Paghman River at Pul-i-Sokhta	-55.1	-9.31	19.38
323	SW	03-24-2007	Paghman River at Pul-i-Sokhta	-56.4	-9.40	18.8
323	SW	04-07-2007	Paghman River at Pul-i-Sokhta	-55.6	-9.44	19.92
323	SW	06-02-2007	Paghman River at Pul-i-Sokhta	-57.2	-9.58	19.44
323	SW	07-02-2007	Paghman River at Pul-i-Sokhta	-55.6	-9.38	19.44
324	SW	12-10-2006	Kabul River at Tangi Saidan	-54.8	-8.92	16.56
324	SW	12-25-2006	Kabul River at Tangi Saidan	-56.9	-9.20	16.7
324	SW	01-10-2007	Kabul River at Tangi Saidan	-55.2	-8.96	16.48
324	SW	01-25-2007	Kabul River at Tangi Saidan	-54.3	-8.98	17.54
324	SW	02-10-2007	Kabul River at Tangi Saidan	-58.8	-9.30	15.6
324	SW	02-24-2007	Kabul River at Tangi Saidan	-54.5	-9.01	17.58
324	SW	03-10-2007	Kabul River at Tangi Saidan	-57.4	-9.21	16.28
324	SW	03-24-2007	Kabul River at Tangi Saidan	-59.3	-9.47	16.46
324	SW	04-07-2007	Kabul River at Tangi Saidan	-58.8	-9.55	17.6
324	SW	04-21-2007	Kabul River at Tangi Saidan	-59.3	-9.64	17.82
987	SW	05-11-2006	Panjshir River at Shukhi	-61.8	-10.13	19.24

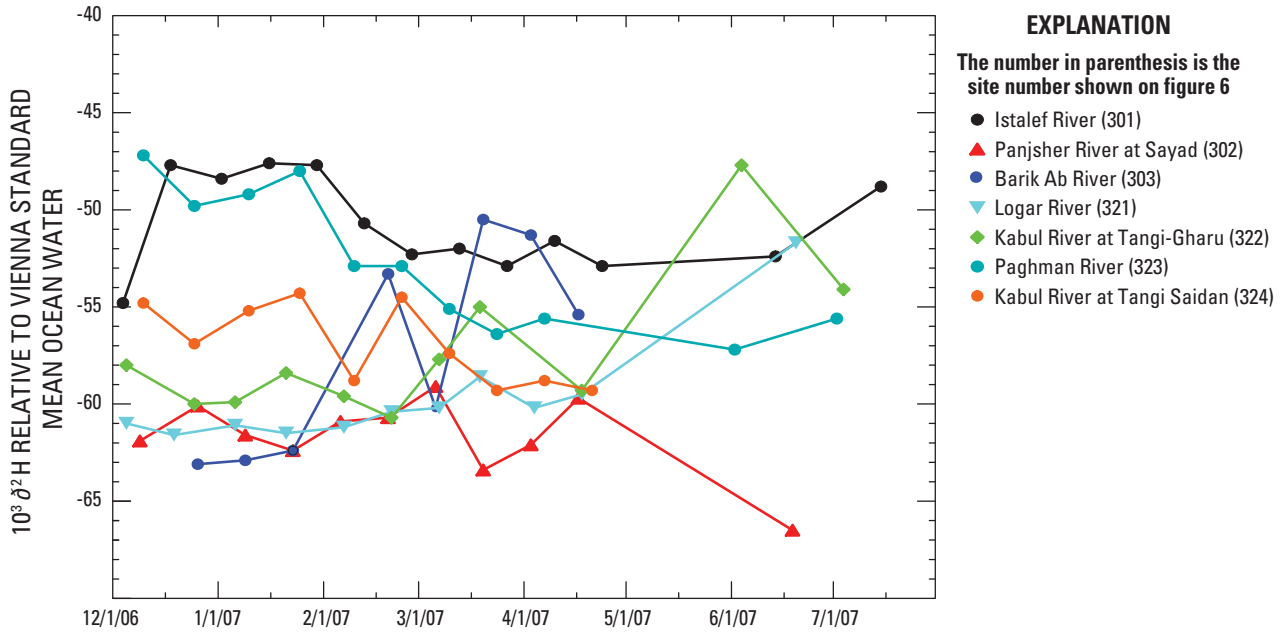


Figure 11-1. Hydrogen isotopic composition, relative to Vienna Standard Mean Ocean Water (VSMOW), of surface water over time in the Kabul Basin, Afghanistan.

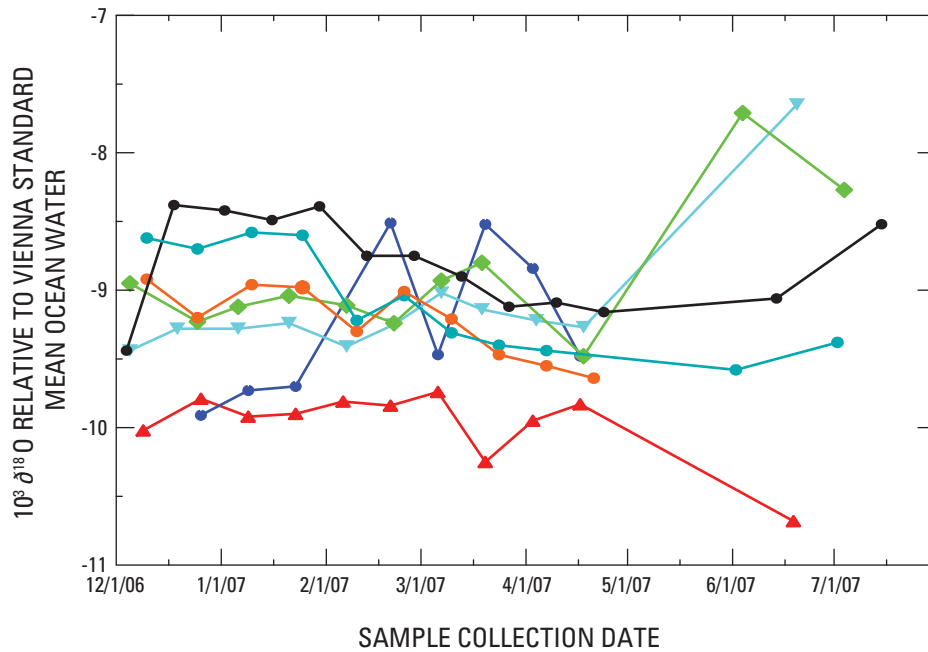


Figure 11-2. Oxygen isotopic composition, relative to Vienna Standard Mean Ocean Water (VSMOW), of surface water over time in the Kabul Basin, Afghanistan.

Table 11-2. Mean deuterium excess, *d*, of selected surface waters.

Station	Site number	10 ³ <i>d</i> Mean	1-σ standard deviation
Paghman River at Pul-i-Sokhta	323	19.91	0.87
Istalef River	301	19.69	0.89
Panjsher River at Sayad	302	18.13	0.68
Kabul River at Tangi Saidan	324	16.86	0.73
Barik Ab River	303	16.77	2.17
Kabul River at Tangi-Gharu	322	13.88	1.19
Logar River at Sang-i-Naweshta	321	13.15	1.51

Groundwater Source Areas

Groundwaters, karezes, and springs are plotted on figure 23, and with few exceptions, they plot near one of the four distinguishable surface-water sources discussed above. Samples from groundwaters, karezes, and springs were separated into seven distinguishable groundwater source areas: Western Front Source Area, Shomali subbasin, Deh Sabz subbasin, Eastern Front Source Area, Paghman and Upper Kabul subbasin, Central Kabul subbasin, and Logar subbasin (table 11-1, fig. 1). Results are plotted and discussed by groundwater source area below.

Western Front

The groundwater and spring sites in the Western Front Source Area are comprised of wells 20, 21, 33, 41, 43, 45, 52, 67, 100 (Swedish well 224), and 104 and spring 101 (fig. 6). Water from these sites is expected to be runoff water, such as rain and snowmelt water from the Paghman Mountains. Examples of such surface water that presumably infiltrates along the western basin flanks are the Istalef River and the Paghman River. In figure 11-3, many of the groundwater samples and one of the spring-water samples lie below the lines for the Istalef River at Istalef and the Paghman River at Paghman samples—their 10³ *d* values range between 16.5 and 18, in accord with groundwater recharge during periods with slightly higher relative humidity than the 70 percent mentioned above. Wells 41, 43, and 45 are along the Istalef River and their δ²H and δ¹⁸O values are in accord with groundwater recharge from this river.

The chloride mass concentrations of samples from the Istalef River at Istalef and the Paghman River at Paghman were in the range of 1 or 2 mg/L at high stage when most groundwater recharge is expected. The chloride mass concentration in Western Front Source Area groundwater ranged from 3 to 18 mg/L with an exceptional value for well 104 of 65 mg/L. If chloride were concentrated in well 104 by evaporation, one would expect to observe a strong enrichment in ²H and ¹⁸O. However, figure 11-3 shows no substantial enrichment in these isotopes, ruling out evaporative enrichment as a mechanism to explain this high chloride concentration.

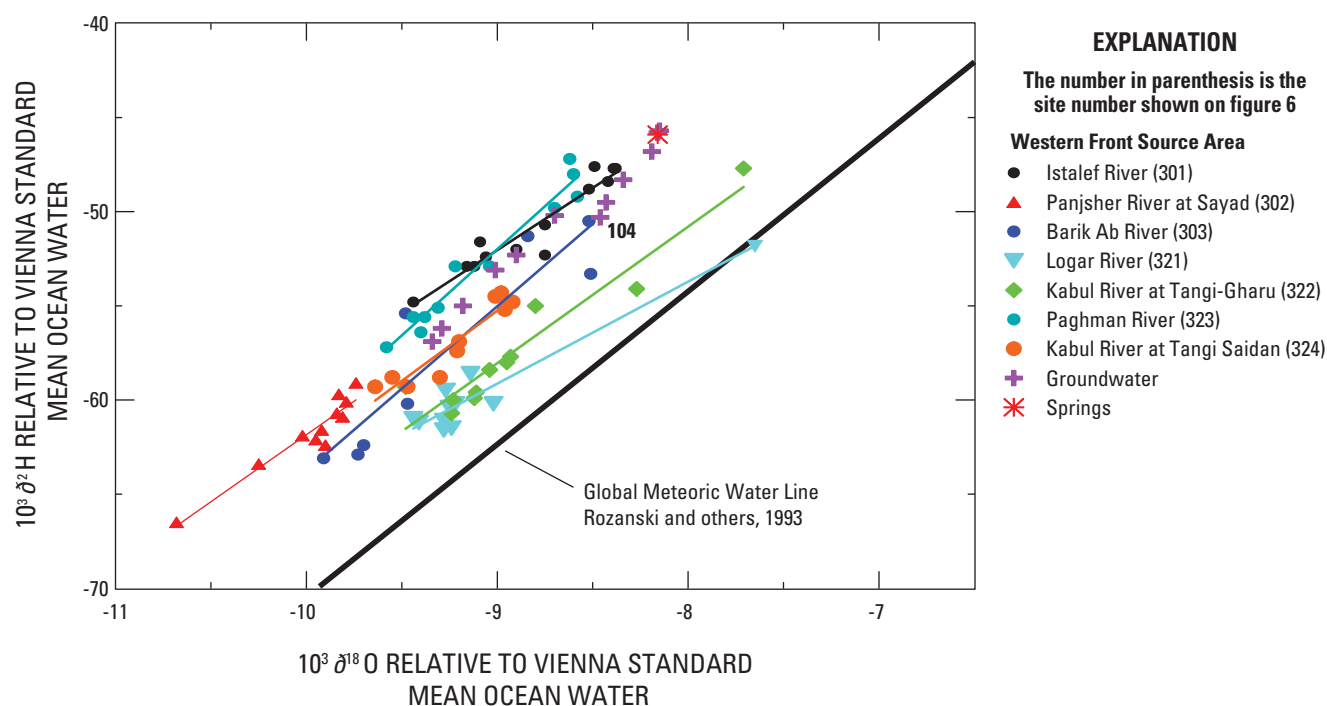


Figure 11-3. The relation between hydrogen and oxygen isotopic composition, relative to Vienna Standard Mean Ocean Water (VSMOW), of all surface waters and of groundwaters and springs in the Western Front Source Area.

Shomali Subbasin

The groundwater and spring sites in the Shomali subbasin are comprised of wells 22.1, 24, 25, 28, 42, 47, 72, and 74 and springs 67A, 67.1 (Kheelre spring), and 68 (fig. 6). Samples from these sites have $10^3 d$ values ranging from 15.3 to 17.7. Although springs 67.2 and 67.1 lie near the Istalef River (figs. 1 and 6), their $10^3 d$ values of 16.54 and 16.02 (fig. 11-1) indicate they were not recharged from modern Istalef River water, which has a $10^3 d$ value of 19.69 ± 0.89 , but from a precipitation source with a relative humidity greater than that which serves as the source area of the Istalef River (fig. 11-4). The same comparison holds for spring 68 and near-by well 52. Well 52 is relatively shallow (23.1 m) and is a good example of a Western Front Source Area with its $10^3 d$ value of 19.5. Spring 68.1, however, reflects a source area with precipitation having higher relative humidity ($10^3 d$ is 16.02) than that for the Western Front Source Area.

The chloride mass concentration in Shomali subbasin ranged from 4 to 18 mg/L with two exceptional values for wells 47 and 74 of 139 and 119 mg/L, respectively. If chloride were concentrated in wells 47 or 74 by evaporation, one would expect to observe a strong enrichment in ^2H and ^{18}O , but figure 11-4 shows no substantial enrichment in these isotopes, ruling out evaporative enrichment as a mechanism to explain these high chloride concentrations.

Deh Sabz Subbasin

The groundwater sites in the Deh Sabz subbasin are comprised of wells 8, 13, 15, 37, and 54 (figs. 1 and 6), and samples from these sites have $10^3 d$ values ranging from 11.3 to 15.2. In figure 11-5, these groundwaters plot closest to the Kabul River at Tang-i-Gharu and Logar River surface-water samples. Some groundwater may flow from the Central Kabul subbasin, through narrow gaps in the interbasin ridge, to the Deh Sabz subbasin.

The chloride mass concentrations of samples from the Kabul River at Tang-i-Gharu and Logar River were in the range of 11 to 19 mg/L at high stage when most groundwater recharge is expected. The chloride mass concentrations of samples from the Deh Sabz subbasin ranged from 29 to 68 mg/L with two exceptional values for wells 8 and 15 of 240 and 315 mg/L, respectively. If chloride were concentrated in wells 8 and 15 by evaporation, one would expect to observe a strong enrichment in ^2H and ^{18}O . Wells 8 and 15 have the highest $\delta^2\text{H}$ and $\delta^{18}\text{O}$ values of the Deh Sabz subbasin (fig. 11-5); thus, enrichment of chloride may be due in part to evaporative enrichment. However, the magnitudes of the enrichment in $10^3 \delta^{18}\text{O}$ are relatively small (approximately 1), which would increase chloride concentration by less than a factor of two. Therefore, other mechanisms are needed to explain the high chloride concentrations in well 8 and 15.

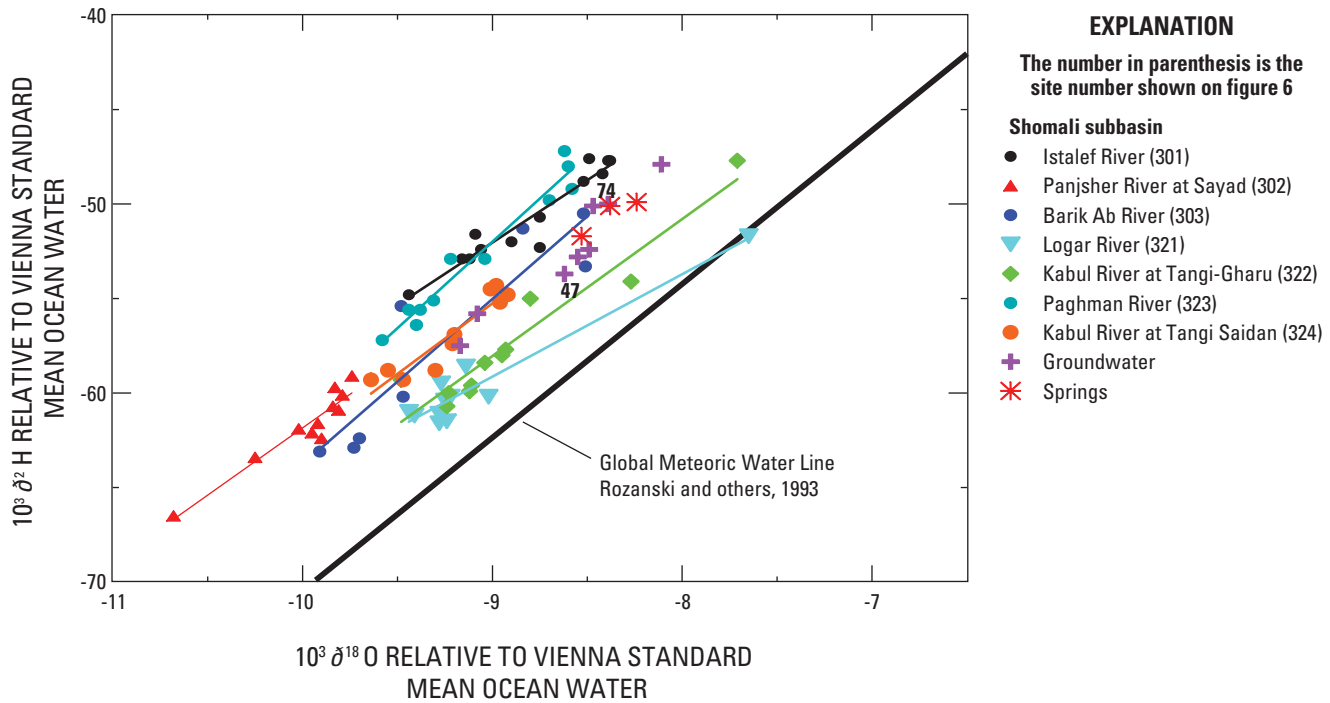


Figure 11-4. The relation between hydrogen and oxygen isotopic composition, relative to Vienna Standard Mean Ocean Water (VSMOW), of all surface waters and of groundwaters and springs in the Shomali subbasin.

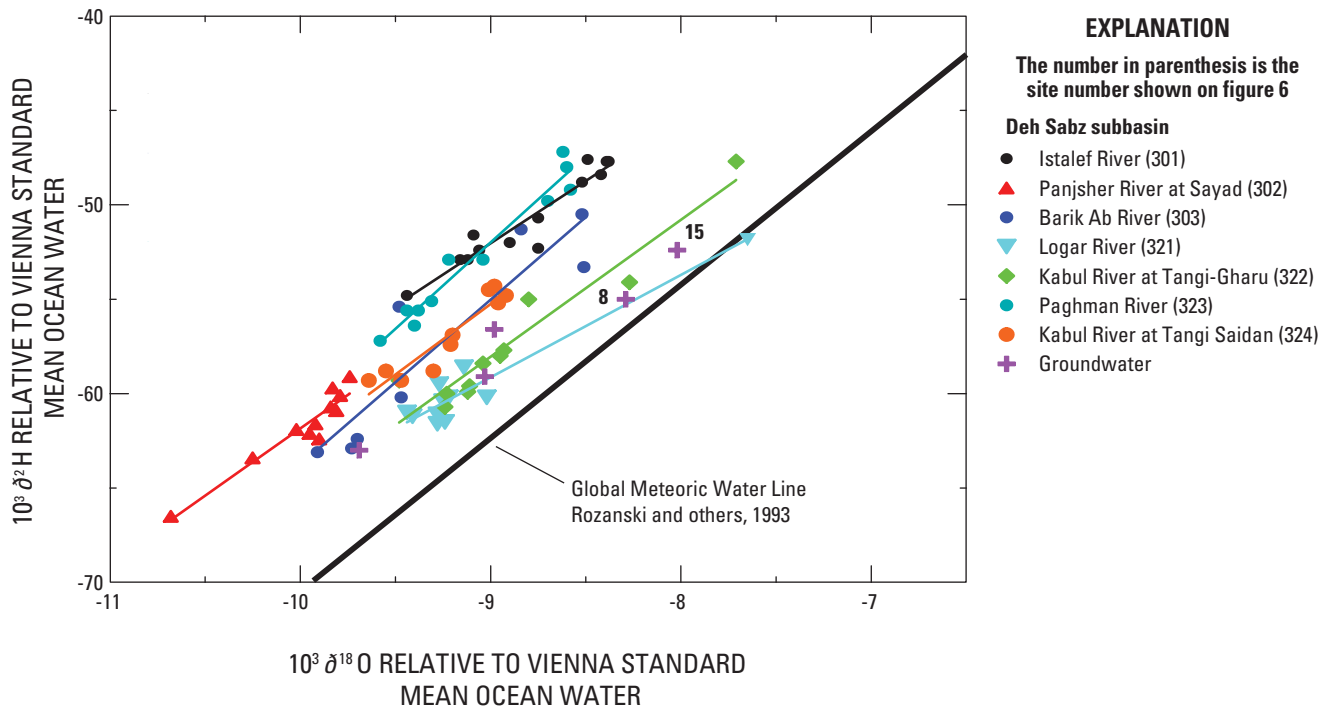


Figure 11-5. The relation between hydrogen and oxygen isotopic composition, relative to Vienna Standard Mean Ocean Water (VSMOW), of all surface waters and of groundwaters and springs in the Deh Sabz subbasin.

Eastern Front

The groundwater, karez, and spring sites in the Eastern Front Source Area are comprised of wells 2.1, 7, 59.1, 71 (Azizi Hotak tank), karez N6, karez 10, karez 69.1, and spring 66.1 (figs. 1 and 6). Samples from these sites had $10^3 d$ values ranging from 18.3 to 21.44. These are expected to be runoff water, such as rain and snowmelt water from the Kohe Safi (fig. 1). These sites are representative of the most arid regions in the Kabul Basin with relative humidity values likely below 70 percent.

The chloride mass concentrations of most of the samples of Eastern Front Source Area were less than 30 mg/L. However, the concentration in well 2.1 was 706 mg/L. If chloride were concentrated in well 2.1 by evaporation, one would expect to observe a strong enrichment in ^2H and ^{18}O , but figure 11-6 shows no substantial enrichment in these isotopes, ruling out evaporative enrichment as a mechanism to explain this high chloride concentration.

Paghman and Upper Kabul Subbasin

The groundwater and karez sites in the Paghman and Upper Kabul subbasin are comprised of wells 107, 112, 113, 115, 117, 182, 184, 211, 212, 213, 214, 216, 217, and 222

(Afshar 6B) and karez 105 (figs. 1 and 6). Samples from these sites had $10^3 d$ values ranging from 12.5 to 16.1, except for values greater than 7.77 for wells 115 and 182 (fig. 11-7). Except for wells 115 and 182, these groundwaters had $\delta^2\text{H}$ and $\delta^{18}\text{O}$ values that were near to those of the Kabul River at Tang-i-Gharu, in good geographic accord. The source of water for wells 115 and 182 appears to be runoff water, such as rain and snowmelt water, similar to that of the Western and Eastern Front Source Areas, based on $10^3 d$ values greater than 17.34. Precipitation in mountains to the west or south are potential sources for these groundwaters. Karez 105 was highly enriched in ^2H and ^{18}O (fig. 11-7) and appears to be a highly evaporated water, not unexpected for a karez.

The chloride mass concentration of the sample from the Kabul River at Tang-i-Gharu was 11 mg/L at high stage when most groundwater recharge is expected. The chloride mass concentrations in samples of groundwater from the Paghman and Upper Kabul area typically were less than 30 mg/L. However, that of well 184 was 103 mg/L. If chloride were concentrated in well 184 by evaporation, a strong enrichment in ^2H and ^{18}O would be expected, but figure 11-7 shows no substantial enrichment in these isotopes, ruling out evaporative enrichment as a mechanism to explain this high chloride concentration.

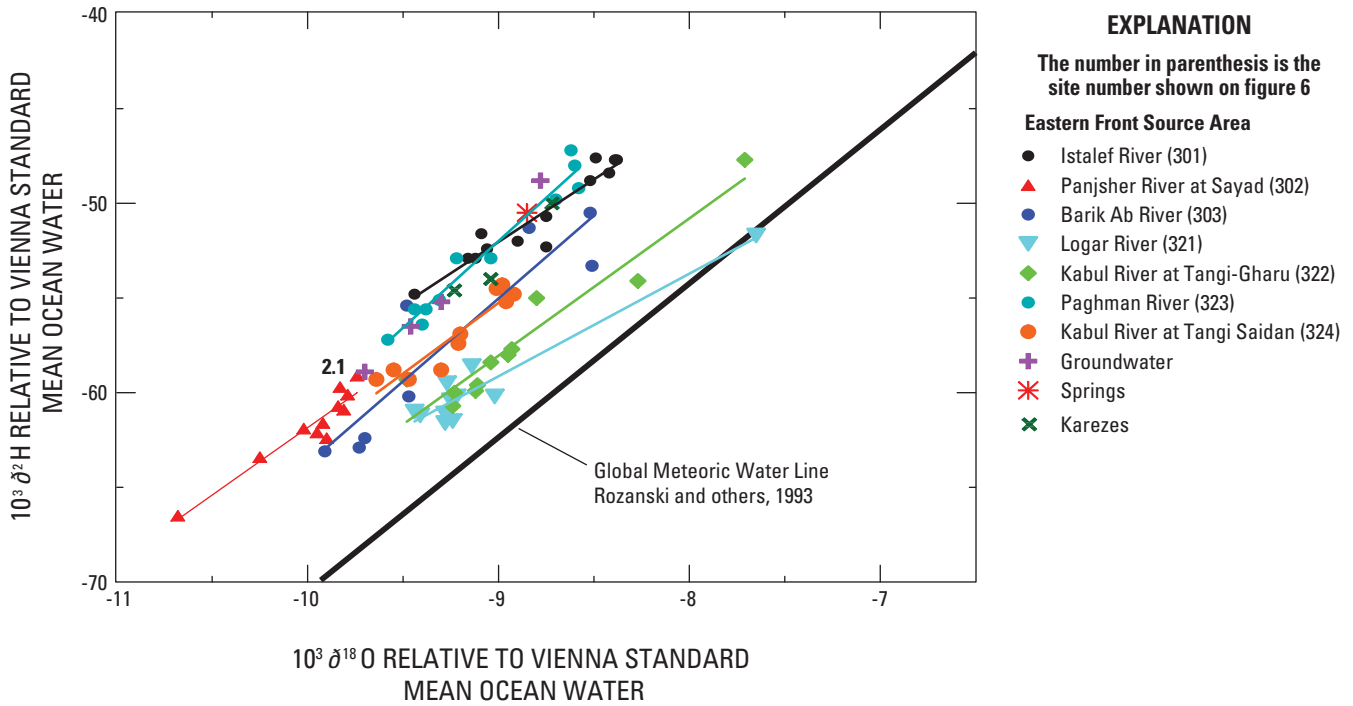


Figure 11-6. The relation between hydrogen and oxygen isotopic composition, relative to Vienna Standard Mean Ocean Water (VSMOW), of all surface waters and of groundwaters and springs in the Eastern Front Source Area.

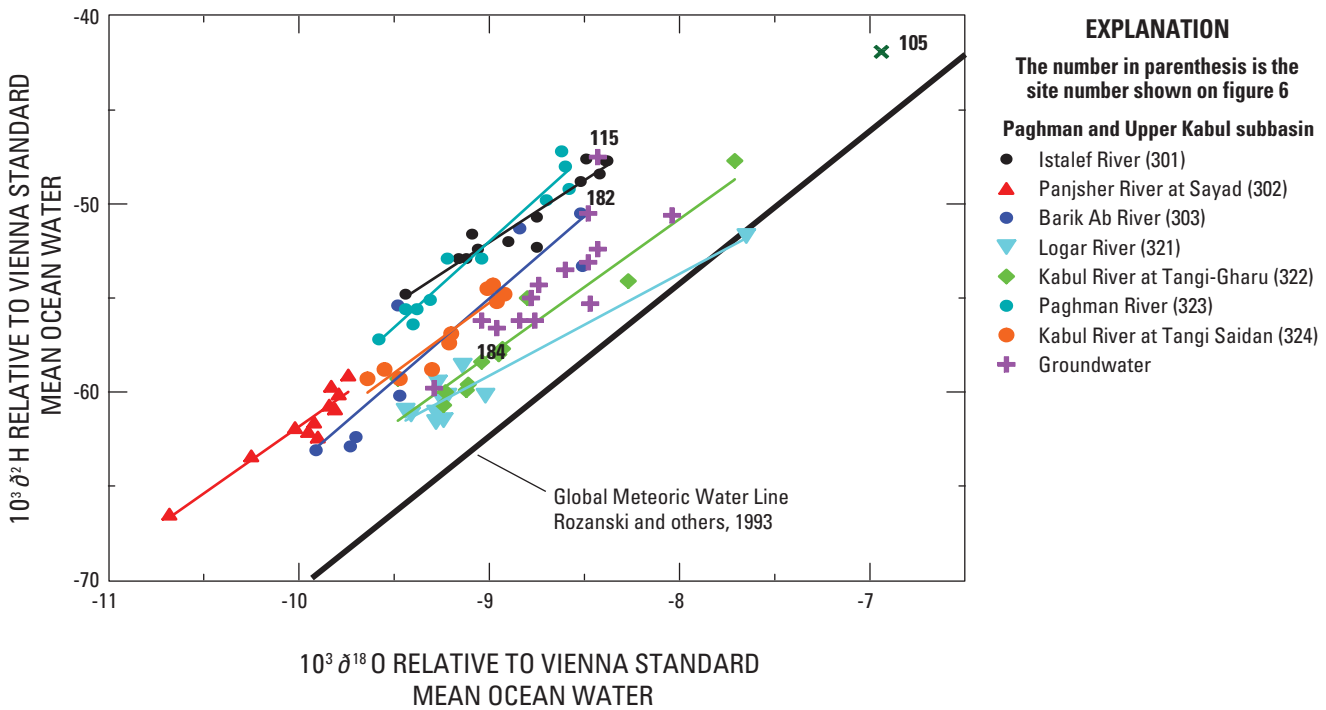


Figure 11-7. The relation between hydrogen and oxygen isotopic composition, relative to Vienna Standard Mean Ocean Water (VSMOW), of all surface waters and of groundwaters and springs in the Paghman and Upper Kabul subbasin.

Central Kabul

The groundwater and spring sites in the Central Kabul subbasin are comprised of wells 64, 65, 124, 129, 133, 148, 152, 153, 156, 157, 162.2, 163, 165, 167, 168, 170, 172, 173, 183 (Hootkel-Nowbahar pump station), 185, 186, 208, 210, 218, 219, 220, and 223 and spring 180 (figs. 1 and 6). Samples from these sites had $10^3 \epsilon_{LC}$ values ranging from -1.2 to 5.8. These sites had δ^2H and $\delta^{18}O$ values that are in excellent accord with values of samples from the Kabul River at Tang-i-Gharu (fig. 11-8).

The chloride mass concentrations of groundwater and spring samples ranged from 22 to 1,650 mg/L, as compared to less than 12 mg/L for high stage Kabul River water that could recharge the groundwater system. If chloride were concentrated by evaporation, one would expect to observe a strong enrichment in 2H and ^{18}O . The two wells with the highest chloride concentrations on which δ^2H and $\delta^{18}O$ measurements were performed are wells 153 and 185 with chloride mass concentrations of 1,650 and 887 mg/L (fig. 11-8). Although the δ^2H and $\delta^{18}O$ values of well 153 are among the most positive of Central Kabul subbasin waters, the magnitude of this enrichment in 2H and ^{18}O is such as to effect less than a doubling in chloride concentration. The δ^2H and $\delta^{18}O$ values of well 184 show no enrichment in 2H and

^{18}O . Therefore, another mechanism is needed to explain the high chloride concentrations in the many of the Central Kabul subbasin groundwaters.

Logar Subbasin

The groundwater and spring sites in the Logar subbasin are comprised of wells 116, 135, 140, 143, 187 (Hotuk Pump Station), 201, 202, 203, 204, and 221 and spring 181 (Chari Sib Spring) (figs. 1 and 6). Samples from these sites had $10^3 \epsilon_{LC}$ values ranging from 0.6 to 5.7. These sites had δ^2H and $\delta^{18}O$ values that are in excellent accord with values of samples from the Logar River (fig. 6), strongly suggesting that this groundwater is Logar River recharged water.

The chloride mass concentrations of samples of Logar subbasin groundwater ranged from 63 to 129 mg/L, compared to 19 mg/L for high-stage Logar River water when most groundwater recharge is expected. Well 116 had the highest chloride mass concentration (129 mg/L) of the Logar subbasin groundwaters. If chloride were concentrated in well 116 by evaporation, a strong enrichment in 2H and ^{18}O would be expected. However, figure 11-9 shows no substantial enrichment in these isotopes in well 116, ruling out evaporative enrichment as a mechanism to explain this high chloride concentration.

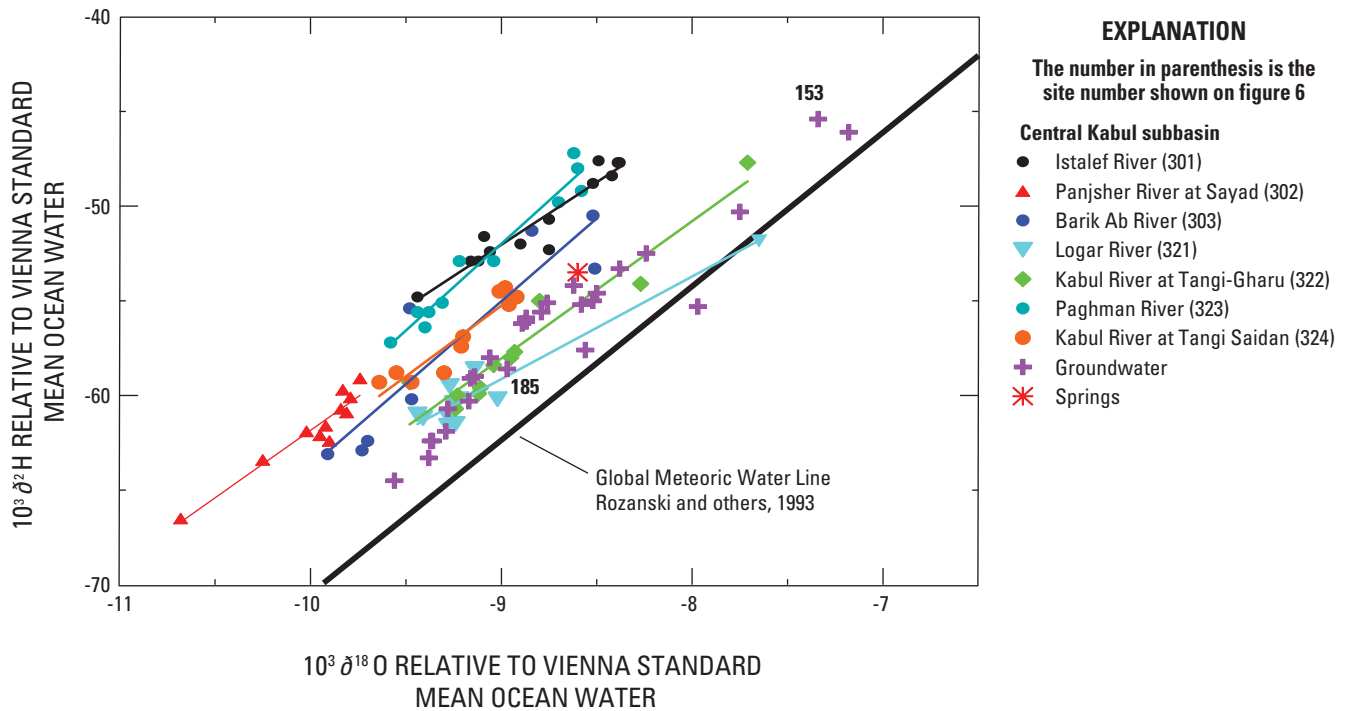


Figure 11-8. The relation between hydrogen and oxygen isotopic composition, relative to Vienna Standard Mean Ocean Water (VSMOW), of all surface waters and of groundwaters and springs in the Central Kabul subbasin.

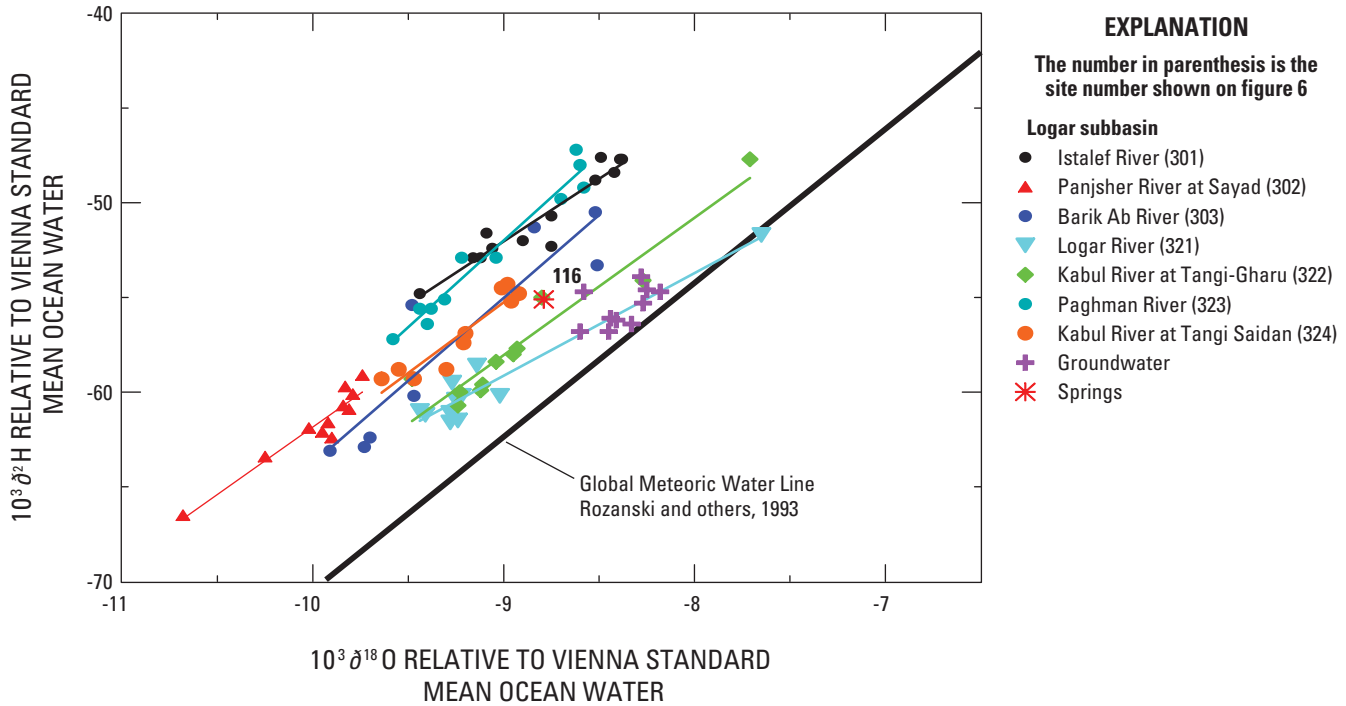


Figure 11-9. The relation between hydrogen and oxygen isotopic composition, relative to Vienna Standard Mean Ocean Water (VSMOW), of all surface waters and of groundwaters and springs in the Logar subbasin.

Summary Observations from Stable-Isotope Data

Several conclusions can be drawn from the stable-isotope data of groundwater and surface water in the Kabul Basin.

1. On the basis of the stable hydrogen and oxygen isotopic compositions, the seven surface-water sites repetitively sampled in this study fall into four distinguishable groups.
 - a. The Istalef River and the Paghman River samples had overlapping isotopic compositions and reflected a precipitation source in an arid environment; their source had the lowest relative humidity (approximately 70 percent) of the four groups.
 - b. The Kabul River at Tang-i-Saidan and the Barik Ab River near Bagram samples formed the second distinguishable region, but the sources areas were geographically distinct.
 - c. The Kabul River at Tang-i-Gharu and the Logar River subbasin samples formed the third distinguishable source.
 - d. The fourth distinguishable source was characterized by Panjsher River samples.
2. The stable hydrogen and oxygen isotope record of IAEA precipitation from Kabul, collected between 1962 and 1989 (with clearly evaporated samples removed), agrees well with that of samples from the Istalef River and the Paghman River, whose source or sources had the lowest relative humidity in the Kabul Basin.
3. Stable hydrogen and oxygen isotopic compositions of surface waters indicate no substantial evaporation.
4. None of the groundwater show substantial evaporation in this arid basin except for a single karez.
5. The groundwater, karez, and spring sites can be divided on the basis of their stable isotopic composition into seven groundwater source areas.
 - a. Western Front Source Area. This groundwater appears to be runoff water, such as rain and snow-melt water from the Paghman Mountains. The relative humidity of the source area or areas is among the lowest in the area (approximately 70 percent).
 - b. Shomali subbasin. This groundwater was not recharged from modern Istalef River water based on isotopic grounds, but from a source having relative humidity higher than ~70 percent.

- c. Deh Sabz subbasin. The $\delta^2\text{H}$ and $\delta^{18}\text{O}$ values of this groundwater plot closest to those of Kabul River at Tang-i-Gharu and Logar River surface water. Some groundwater may flow through gaps in interbasin ridges from the Central Kabul subbasin to the Deh Sabz subbasin.
 - d. Eastern Front Source Area. The origin of this water, adjacent upland mountains, is similar to that of the Western Front Source Area. The relative humidity of the source area is among the lowest in the region (approximately 70 percent).
 - e. Paghman and Upper Kabul subbasin. Except for wells 115 and 182, this groundwater has $\delta^2\text{H}$ and $\delta^{18}\text{O}$ values that are near to those of the Kabul River at Tang-i-Gharu surface water, in good geographic accord.
 - f. Central Kabul subbasin. This groundwater has $\delta^2\text{H}$ and $\delta^{18}\text{O}$ values that are in excellent accord with those of the Kabul River at Tang-i-Gharu surface water, the presumed source.
 - g. Logar subbasin. This groundwater appears to be derived from the Logar River on the basis of the similarity of the $\delta^2\text{H}$ and $\delta^{18}\text{O}$ values.
6. A small fraction of wells throughout the Kabul Basin have chloride concentrations a factor of 10 to at least 50 higher than their presumed source water. The lack of substantial enrichment in ^2H and ^{18}O in these higher chloride waters indicates that evaporation did not cause this chloride enrichment.

References Cited

- Clark, I.D., and Fritz, P., 1997, *Environmental Isotopes in Hydrogeology*: Lewis Publishers, Boca Raton, Fla., 352 p.
- Dansgaard, W., 1964, Stable isotopes in precipitation: *Tellus*, v. 16, p. 436–468.
- Merlivat, L., and Jouzel, J., 1979, Global climatic interpretation of the deuterium–oxygen-18 relationship for precipitation: *Journal of Geophysical Research*, v. 84, p. 5029–5033.
- Rozanski, K., Araguas-Araguas, L., Gonfiantini, R., 1993, Isotopic patterns in modern global precipitation, *Climate Change in Continental Isotopic Records*, Geophysical Monograph 78, Swart, P.K., Lohmann, K.C., McKenzie, J., and Savin, S., eds: American Geophysical Union, Washington, D.C., (1993), p. 1–36.

This page intentionally left blank.

Appendix 12. Water Chemistry, Geochemical Reactions, and Solute Origins

Contents

Water chemistry, geochemical reactions, and solute origins.....	204
Solute ratios.....	205
Conservative solutes.....	206
Reactive solutes.....	207
Tritium and Chlorofluorocarbons.....	207
Uptake of water by vegetation (transpiration).....	207
References cited.....	208

Figures

Figure 12-1. Mass concentrations of dissolved (A) calcium, (B) alkalinity as CaCO_3 , (C) silica, and (D) arsenic in surface water and groundwater from the Kabul Basin as a function of dissolved chloride mass concentration. It is likely that CaCO_3 precipitated in bottles prior to determination of alkalinity for many of the PASSPORT water samples, and for water from the Japan International Corporation Agency TW-1 sample.....	204
Figure 12-2. Mass concentrations of dissolved (A) sulfate, (B) magnesium, (C) sodium, and (D) potassium in surface water (blue), shallow groundwater (red), and deep groundwater (green and purple) from the Kabul Basin as a function of dissolved chloride mass concentration. The PASSPORT wells in (C) show the quantity Na+K; K was not determined separately for water from the PASSPORT wells.....	205
Figure 12-3. The hydrogen versus oxygen isotopic composition of surface water, groundwater, and water from karezes and springs in the Kabul Basin, Afghanistan.....	206
Figure 12-4. Mass fractions of CFC-12 (A) and tritium (B) in surface water and groundwater from the Kabul Basin as a function of dissolved chloride mass concentration.....	208

Appendix 12. Water Chemistry, Geochemical Reactions, and Solute Origins

Most of the groundwater samples collected as a part of this investigation were from relatively shallow sources (depths of 5–185 m, median depth of 48 m (data provided in appendix 10). Deeper wells drilled by the former USSR in the 1970s, known as PASSPORT wells, have depths of 172 to 654 m (median depth of 267 m), and one recently drilled test well (Japan International Cooperation Agency, TW-1) reaches a depth of 640 m (Japan International Cooperation Agency, 2007a, b). The compositions of these waters from relatively deep sources are compared and contrasted with the relatively shallow groundwater samples of this study in figure 12-1. The dissolved solute concentrations of the

deep and shallow groundwater samples overlap but tend to be somewhat more elevated in the deep samples than in the shallow groundwater samples. The maximum and median chloride mass concentrations of the shallow wells were nearly 4,190 and 56 mg/L in groundwater in the Kabul Basin (Central Kabul subbasin), and the maximum and median chloride concentrations of the deeper PASSPORT and JICA TW-1 samples were 7,091 and 237 mg/L, respectively. The origin/source/cause of the elevated solute concentration of groundwater of the Kabul Basin needs to be understood in order to distinguish recharge sources to the Basin. Several hypotheses for the origin of the elevated solute concentration were considered: (1) evaporation of surface water (2) geochemical water-rock reactions, (3) dissolution of salts precipitated from evaporation of surface water, (4) upward leakage of (presumed) deep saline water, and (5) water uptake by vegetation.

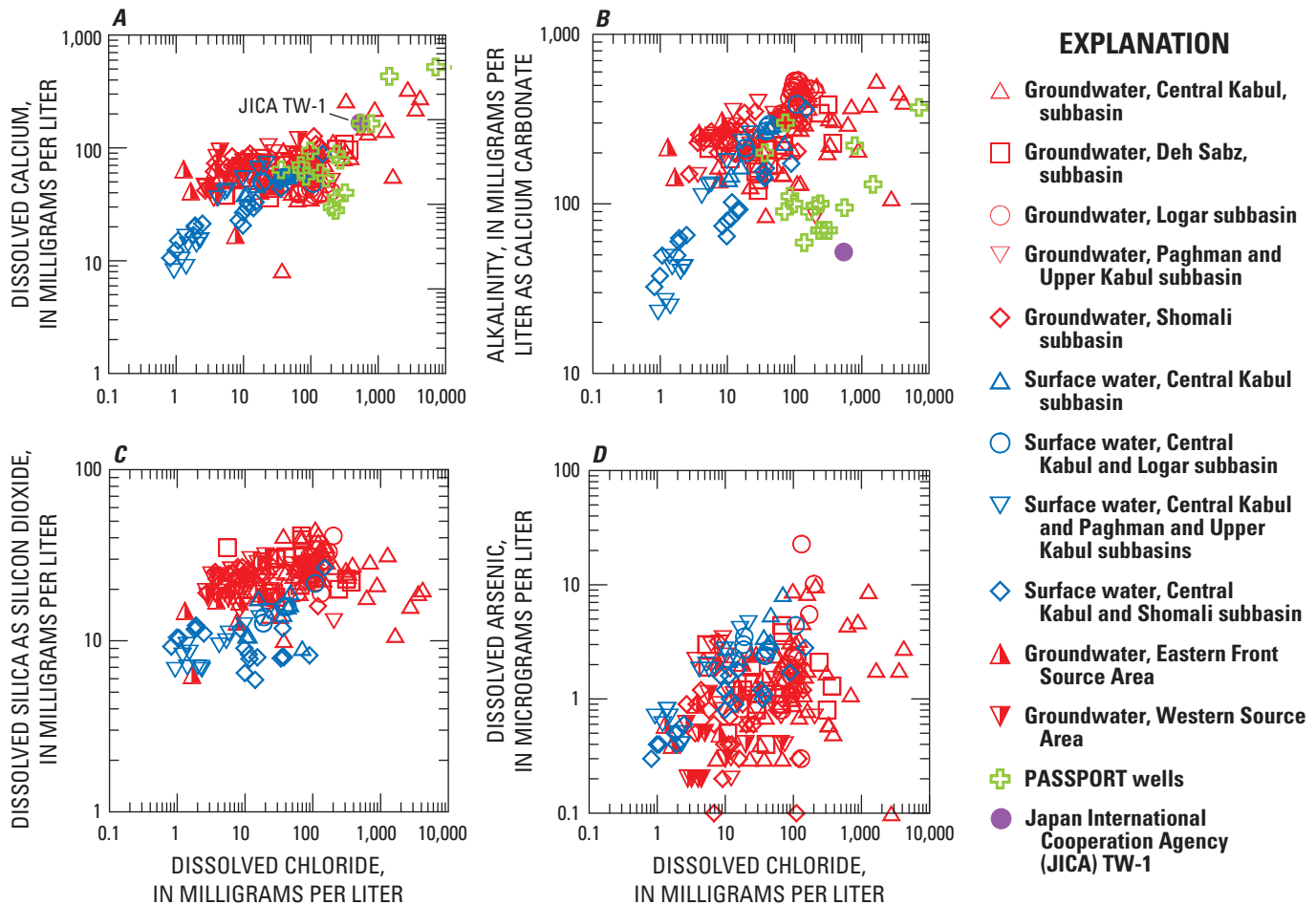


Figure 12-1. Mass concentrations of dissolved (A) calcium, (B) alkalinity as CaCO_3 , (C) silica, and (D) arsenic in surface water and groundwater from the Kabul Basin as a function of dissolved chloride mass concentration. It is likely that CaCO_3 precipitated in bottles prior to determination of alkalinity for many of the PASSPORT water samples, and for water from the Japan International Cooperation Agency TW-1 sample.

Solute Ratios

The average ratios of the mass concentrations of some of the major dissolved solutes (particularly Na and SO₄, and to some extent that of Mg) to that of dissolved chloride in groundwater are near those average ratios in surface water for the subbasin and plot along mass concentration trend lines similar to that of surface water (fig. 12-2). This pattern of solute mass concentrations relative to dissolved chloride (fig. 12-2) observed in the relatively shallow groundwater samples (median depth 48 m) of this study continues to waters of more than 650 m depth in the Kabul Basin (Japan

International Cooperation Agency, 2007a, b). The similarity in solute ratios in surface water and groundwater for Na/Cl, SO₄/Cl and to some extent Mg/Cl suggests a surface-water source for groundwater with subsequent concentration by evapotranspiration processes. But as explained above in discussion of the stable-isotope data (appendix 11), there is little or no evidence of isotopic fractionation of stable isotopes of water (fig. 12-3), and it is unlikely that evaporative concentration of surface water can be invoked to explain the elevated dissolved solute concentrations. More likely, the water is removed by the non-fractionating process of transpiration by plants.

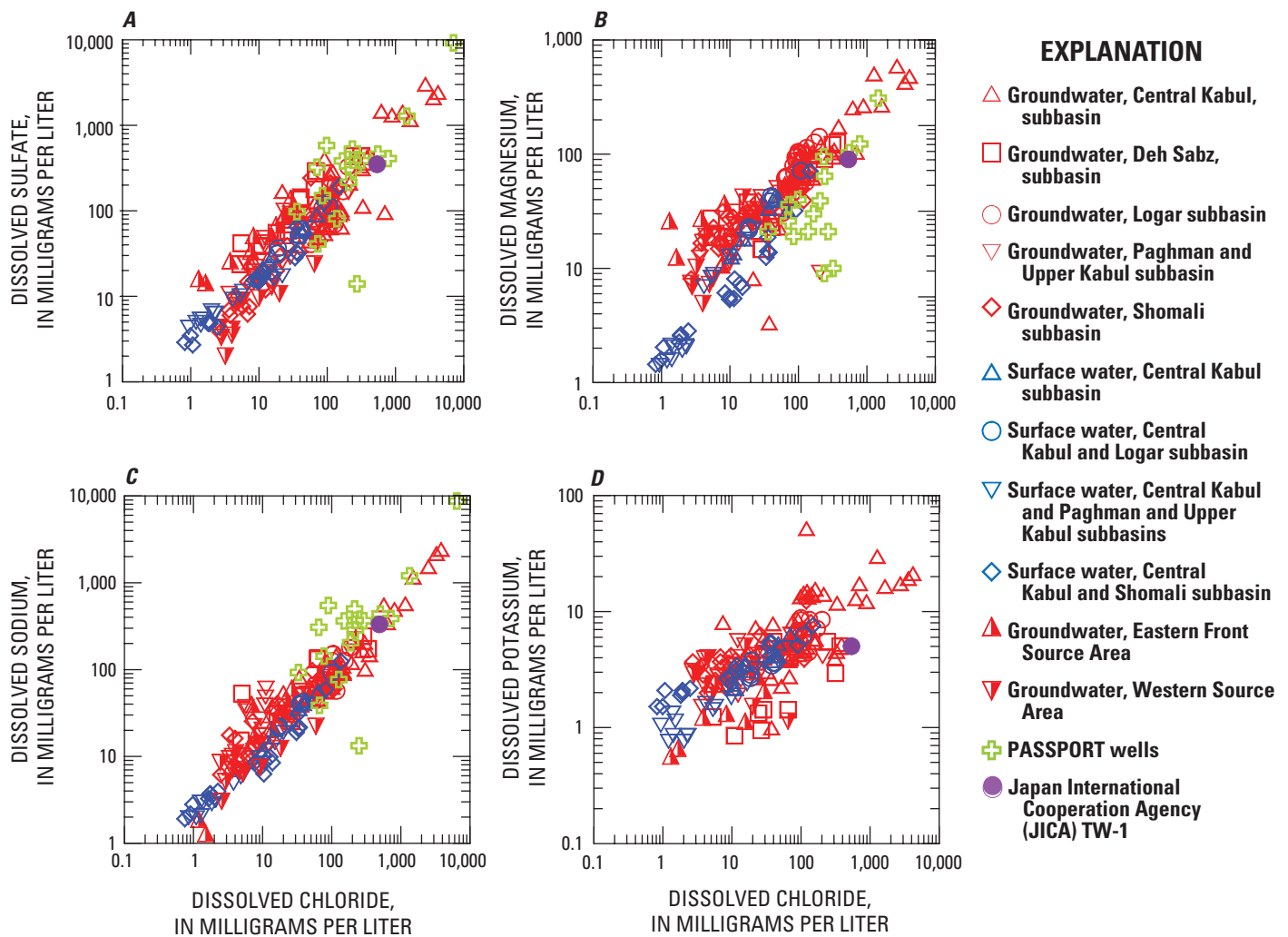


Figure 12-2. Mass concentrations of dissolved (A) sulfate, (B) magnesium, (C) sodium, and (D) potassium in surface water (blue), shallow groundwater (red), and deep groundwater (green and purple) from the Kabul Basin as a function of dissolved chloride mass concentration. The PASSPORT wells in (C) show the quantity Na+K; K was not determined separately for water from the PASSPORT wells. (This figure is the same as figure 24).

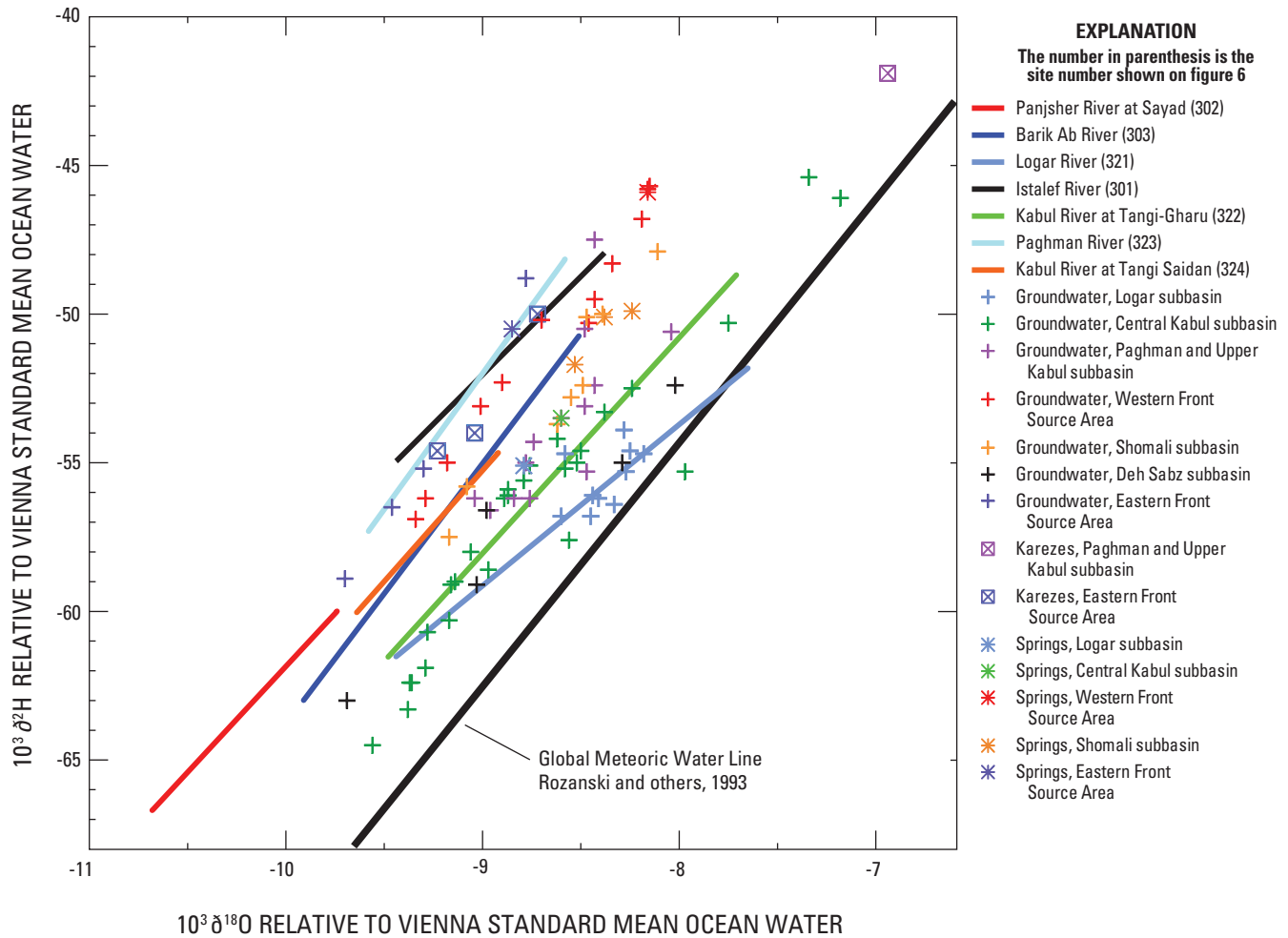


Figure 12-3. The hydrogen versus oxygen isotopic composition of surface water, groundwater, and water from karezes and springs in the Kabul Basin, Afghanistan. (This figure is the same as figure 23).

Conservative Solute

Because the average ratios of mass concentrations of sodium, sulfate, and to some extent magnesium to chloride are similar to those average mass concentration ratios in surface water, it is unlikely that dissolution of evaporative salts would result in the same solute ratios (fig. 12-2). Other geochemical processes also appear not to affect the water chemistry. For example, the linear relation between dissolved chloride and sulfate (fig. 12-2A) eliminates, for most of the samples, reactions that can remove sulfate (such as microbially mediated sulfate reduction) or add sulfate (oxidation of sulfide minerals, dissolution of gypsum). One sample from a deep PASSPORT well (fig. 12-2A) may have undergone sulfate reduction, lowering the sulfate to chloride ratio in that sample. Waters from JICA TW-1 and the PASSPORT wells are similar in ratio and solute concentration to many of the relatively shallow groundwater samples of the Kabul Basin (fig. 12-2). The dissolved magnesium to chloride relation in groundwaters and surface waters (fig. 12-2B) indicates that

dolomite dissolution is probably not an important water-rock reaction in groundwaters of the Kabul Basin, otherwise, the Mg/Cl ratio (ratio of Mg mass concentration to Cl mass concentration) would increase with dissolved chloride concentration along a trend line exceeding that for the surface waters. However, some small differences in the magnesium-chloride concentrations of surface waters probably reflect differences in mineralogy in the source areas (fig. 12-2B). The linear relation of magnesium to chloride in groundwaters suggests that there are no important geochemical reactions that add or remove magnesium from the shallow groundwater and most of the deep groundwater samples (fig. 12-2B). However, approximately half of the PASSPORT samples have somewhat lower Mg/Cl ratios than observed in the JICA TW-1 sample and in the more shallow Kabul Basin samples. These waters may have a different origin or may be affected by geochemical processes that remove Mg from groundwater, because of dolomitization or cation-exchange reactions. However, the linear relation in dissolved sodium and chloride (fig. 12-2C) indicates that cation exchange is not a major water-rock

reaction in the region. Most of the potassium concentrations are similar to those of surface waters, or conservatively concentrated surface waters, eliminating possible water-rock reactions involving potassium in forming groundwater compositions (fig. 12-2D). Other dissolved solutes in groundwaters that show nearly constant ratios to dissolved chloride include bromide, boron, and strontium, suggesting little or no water-rock reaction involving these solutes.

Reactive Solutes

Several other dissolved solute to dissolved chloride ratios suggest some geochemical reactions may be occurring, but these cannot account for the elevated solute concentrations. Somewhat elevated calcium, magnesium, and alkalinity relative to chloride in some of the more dilute groundwater samples suggest dissolution of dolomite (figs. 12-2B and 12-1A,B) may occur in some samples. Lower calcium and alkalinity concentrations with increasing dissolved chloride concentration suggest precipitation of calcium carbonate (most likely calcite) (fig. 12-1A,B) in some samples. Most of the groundwater has elevated silica concentrations relative to that of surface water as a function of dissolved chloride (fig. 12-1C) reflecting, possibly, dissolution of primary silicate minerals or other siliciclastics that are abundant in the rocks and alluvial deposits of the Kabul Basin. Most of the dissolved arsenic concentrations in groundwater are less than those of surface water as a function of dissolved chloride (fig. 12-1D). If surface water is the primary source of arsenic to groundwater, arsenic appears to be partially removed by geochemical processes in the groundwater environment—probably by sorption on iron-manganese oxyhydroxides. The presence of dissolved oxygen in many of the groundwater samples and lack of evidence of sulfate reduction suggest removal of arsenic as sulfides is not occurring. A few other reactions are noted from comparing solute concentrations to dissolved chloride, and these include limited formation of barite and fluorite in the more concentrated samples, a lowering of dissolved lithium in some waters from the Deh Sabz region, and a lowering of dissolved manganese concentrations relative to chloride in some waters, presumably because of the formation of iron-manganese oxyhydroxides.

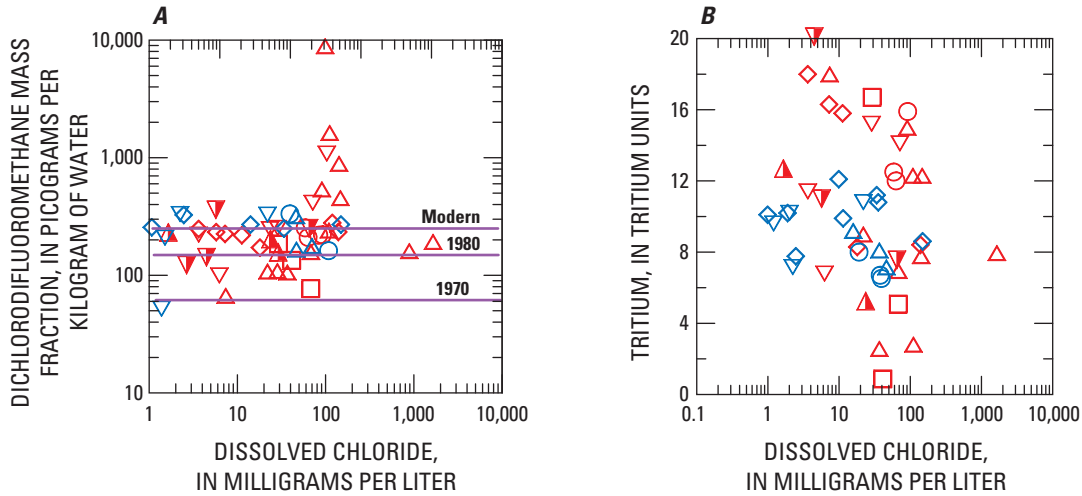
Tritium and Chlorofluorocarbons

Relatively few of the samples analyzed for dissolved solutes were analyzed for chlorofluorocarbons and tritium (43 total), and of these, all samples contained CFCs and tritium (fig. 12-4); even those samples with nearly 2,000 mg/L of dissolved chloride contained CFCs and tritium. Most of the groundwater samples had CFC-12 volume fractions consistent with recharge of post-1970s water (fig. 12-4A). Leakage of saline waters into the basin as a source of the elevated solutes is unlikely because the saline source, being presumably from old deep-basin groundwater, would have to contain major

amounts of tritium and chlorofluorocarbons, which is unlikely for old groundwater. Further, the saline water would have to have cation/anion mass ratios similar to that of the surface waters. Still, the possibility of mixtures of old, tracer-free saline water with a young fraction cannot be completely ruled out, though both fractions would have to have similar cation/anion mass ratios.

Uptake of Water by Vegetation (Transpiration)

It appears that the source of solutes in most of the sub-regions of the Kabul Basin was surface water, as supported further by the stable-isotope data (appendix 11). Many of the groundwater samples had solute concentrations that exceeded those measured in surface water by factors of as much as 100 or more. However, these samples were not likely evaporated because there was no evaporative trend in stable-isotope composition (figs. 11-3 to 11-9). Apparently, the elevated solute concentration of the groundwater can be attributed to transpiration along the rivers and surface-water drainage, and near irrigated crop land, wherever plant root systems can reach the water table. Because all the groundwater samples contained CFCs and tritium, even those with dissolved chloride mass concentrations of as much as 2,000 mg/L, the transpiration process is widespread in irrigated areas where most of the wells sampled for this study are located and is occurring on the anthropogenic timescale (the past 60 years). On the basis of the chemical, stable-isotope, and environmental-tracer data, it is concluded that infiltration of surface water, with subsequent concentration through transpiration, was the most likely source of recharge for most of the groundwater of the various subbasins of the Kabul Basin sampled as a part of this investigation. In irrigated agricultural areas where pumps are used to extract groundwater, water may be utilized through multiple cycles of pumping, irrigation, and return flow to the water table, further elevating the dissolved solute concentration. Table 6 summarizes average solute concentrations, stable isotope data, and tritium data for groundwater from the seven groundwater regions and compares average solute concentrations in groundwater to average values from surface water in each region. The average values of specific conductance of groundwater were 2,200, 1,150, 500, 1,300, 700, 700, and 500 $\mu\text{S}/\text{cm}$ at 25°C for the Central Kabul subbasin, Deh Sabz subbasin, Eastern Front Source Area, Logar subbasin, Paghman and Upper Kabul subbasin, Shomali subbasin, and Western Front Source Area, respectively. The average values of specific conductance of surface water for the Central Kabul, Logar, Paghman and Upper Kabul, and Shomali subbasins were about 660, 660, 290, and 320, respectively (no surface-water samples were obtained from the Deh Sabz subbasin). The average surface-water solute mass concentrations are increased during irrigation and infiltration cycles relative to those of local surface water by factors of 3.3, 1.9, 2.5, and 2.2 for the Central Kabul, Logar, Paghman and Upper Kabul, and Shomali subbasins, respectively.



EXPLANATION

- ▲ Groundwater, Central Kabul subbasin
- Groundwater, Deh Sabz subbasin
- Groundwater, Logar subbasin
- ▽ Groundwater, Paghman and Upper Kabul subbasin
- ◇ Groundwater, Shomali subbasin
- △ Surface water, Central Kabul subbasin
- Surface water, Logar subbasin
- ▽ Surface water, Paghman and Upper Kabul subbasin
- ◇ Surface water, Shomali subbasin
- ▲ Groundwater, Eastern Front Source Area
- ▼ Groundwater, Western Front Source Area

Figure 12-4. Mass fractions of CFC-12 (A) and tritium (B) in surface water and groundwater from the Kabul Basin as a function of dissolved chloride mass concentration.

References Cited

Japan International Cooperation Agency (JICA), 2007a, The study on groundwater resources potential in Kabul Basin, in the Islamic Republic of Afghanistan: 3rd Joint Technical Committee, Sanyu Consultants, Inc., Kabul, Afghanistan, p. 20.

Japan International Cooperation Agency (JICA), 2007b, The study on groundwater resources potential in Kabul Basin, in the Islamic Republic of Afghanistan: 4th Joint Technical Committee, Sanyu Consultants, Inc., Kabul, Afghanistan, p. 12.

Appendix 13. Interpretations of Water Age Based on CFCs and Tritium Data

Contents

Interpretations of water age based on CFCs and tritium data	210
Age interpretation.....	210
Atmospheric input functions of CFCs and tritium for the Kabul Basin.....	215
CFCs	215
Tritium	215
CFCs in groundwater	215
CFCs in surface water and air	216
CFC ages.....	216
Age variations between groundwaters	216
Age gradients in groundwater.....	222
Comparison of CFC and tritium data	227
References cited.....	229

Figures

Figure 13-1. Volume fraction of CFCs (CFC-11, CFC-12, CFC-113) in North American (N.A.) air, 1940 to 2007, in ppt, and tritium in precipitation reconstructed for the Kabul Basin and vicinity (see text) decayed to the date, 2006, in tritium units, TU	210
Figure 13-2. Tracer-Tracer plots comparing volume fractions of CFCs in groundwater, water from springs, surface water, and air in the Kabul Basin	217
Figure 13-3. CFC-11 piston-flow ages in the Kabul Basin, Afghanistan	223
Figure 13-4. CFC-12 piston-flow ages in the Kabul Basin, Afghanistan	224
Figure 13-5. CFC-113 piston-flow ages in the Kabul Basin, Afghanistan	225
Figure 13-6. Apparent (piston-flow) ages as a function of depth below the water table	226
Figure 13-7. Tracer-Tracer plots comparing tritium and CFC volume fractions in groundwater, water from springs, and surface water in the Kabul Basin.....	228

Tables

Table 13-1. Chlorofluorocarbon and tritium data collected in the Kabul Basin, Afghanistan.....	211
Table 13-2. Summary of dissolved gas composition of selected groundwater samples, estimated excess N_2 from denitrification, estimated recharge temperature and estimated quantity of excess air in the Kabul Basin, Afghanistan	218
Table 13-3. Summary of piston-flow and binary mixing model ages of groundwater and spring water based on chlorofluorocarbon data in the Kabul Basin, Afghanistan.....	219
Table 13-4. Summary of average ages, percentages of young water, and percentages of modern water, based on concentrations of chlorofluorocarbons and tritium in groundwater and water from springs by subbasin and source area in the Kabul Basin, Afghanistan.....	222

Appendix 13. Interpretation of Water Age Based on CFCs and Tritium Data

Age Interpretation

Age interpretation based on CFCs and tritium uses historical records of volume fractions of CFCs in air and of ³H in local precipitation (fig. 13-1) and depends on choice of the appropriate mixing model to apply to the hydrologic setting. Four hypothetical mixing models were considered—piston flow, exponential mixing, exponential-piston flow, and binary mixing (Cook and Böhlke, 1999). These models commonly describe the range of variations in mixing seen in groundwater environments. Possible mixing relations among the volume fractions of CFC-11, CFC-12, CFC-113 and of ³H were evaluated by comparing the volume fractions calculated from the measured mass concentrations (table 13-1) with the expected volume fractions according to various mixing models.

Water reaching the open interval of wells with narrow openings or discharging at shallow water-table springs can be nearly uniform in age and can be approximated using a piston-flow model (unmixed water). In this case, amounts of environmental tracer in the water sample closely correspond to amounts in recharge water for the time of recharge. Unmixed samples would have volume ratios close to those of figure

13-1 for the corresponding year of recharge. As tritium undergoes radioactive decay, the sample year is assumed to be 2006, accounting for the decay of tritium in precipitation to the sample year. Exponential mixing can describe discharge from an unconfined aquifer receiving uniform aerial recharge (Eriksson, 1958; Vogel, 1967; Maloszewski and Zuber, 1982; Maloszewski and others, 1983). The exponential model could apply to discharge from wells with relatively large open intervals that integrate a range of water ages or water from springs that discharge from a large groundwater reservoir. The exponential-piston flow model can describe discharge from wells or springs in aquifers, initially unconfined (exponential mixing), that become confined over their aerial extent. In the calculations considered here, the proportion of unconfined and confined aerial extent was assumed to be 1:1, as an example. The binary mixing model applies best in some fractured-rock aquifers where the young (tracer-bearing) component is diluted with old (low- or zero-tracer amount) water. The mean age of the young fraction is calculated from the ratio of the volume fractions of two CFC tracers. The values are calculated from the measured mass concentrations in water and the Henrys Law solubility constant at the altitude and temperature of the sample during recharge. In the case of binary mixing, volume ratios of CFC values define the mean age of the young fraction and, if diluted with old, tracer-free water, the measured CFC mass concentrations can define the fraction of young water in the mixture (International Atomic Energy Agency, 2006).

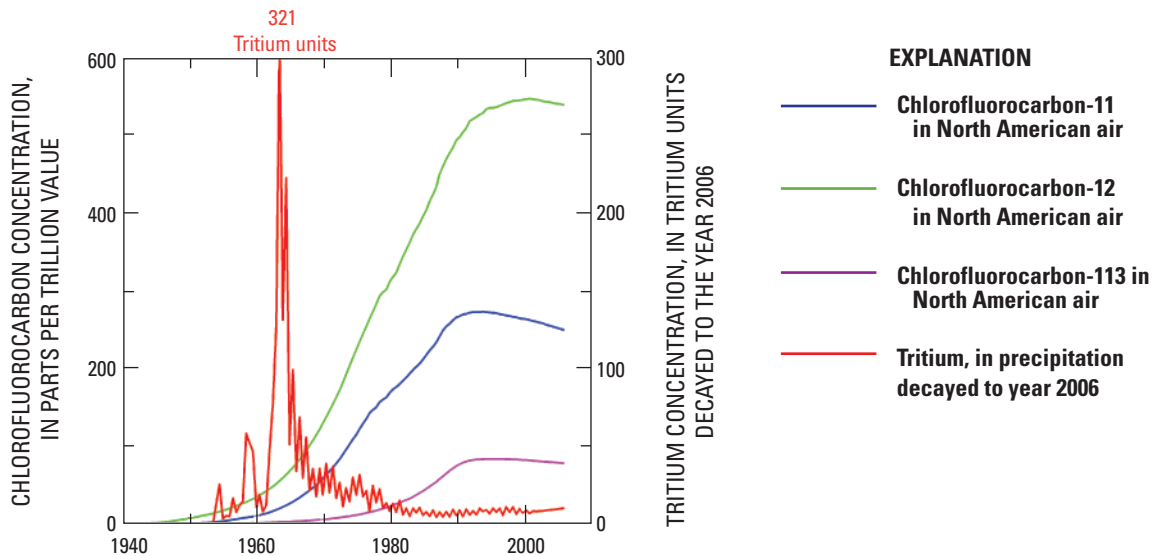


Figure 13-1. Volume fraction of CFCs (CFC-11, CFC-12, CFC-113) in North American (N.A.) air, 1940 to 2007, in ppt, and tritium in precipitation reconstructed for the Kabul Basin and vicinity (see text) decayed to the date, 2006, in tritium units, TU.

Table 13-1. Chlorofluorocarbon and tritium data collected in the Kabul Basin, Afghanistan.

[CFC, Chlorofluorocarbon; CFC-11, trichlorofluoromethane; CFC-12, dichlorodifluoromethane; CFC-113, trichlorotrifluoroethane; pg kg⁻¹, picograms per kilogram; ppt, parts per trillion; TU, Tritium Unit; nd, not determined]

Site number	Name	Groundwater region	Sample date	Sample time	CFC-11 mass fraction ¹ , pg/kg	CFC-12 mass fraction ¹ , pg/kg	CFC-113 mass fraction ¹ , pg/kg	CFC-11 volume fraction ¹ , ppt	CFC-12 volume fraction ¹ , ppt	CFC-113 volume fraction ¹ , ppt	CFC-11 fraction modern ²	CFC-12 fraction modern ²	CFC-113 fraction modern ²	Tritium, in TU
13	Pacha Sahab	Deh Sabz	05-16-2006	1200	246.2	184.8	29.6	123.2	395.0	35.4	49.9	73.1	45.5	16.7
28	Obchakan Ball	Shomali	05-23-2006	1300	424.2	218.7	55.6	209.3	460.7	65.6	84.8	85.3	84.5	15.8
33	Mir Afghan	Western Front	05-23-2006	1030	202.7	142.2	20.3	102.7	307.6	24.5	41.6	57.0	31.6	20.1
37	Shekhu	Deh Sabz	05-14-2006	1000	194.8	133.9	32.8	95.9	281.4	38.5	38.8	52.1	49.6	0.9
42	Godar	Shomali	05-28-2006	0810	308.6	171.7	38.6	149.5	355.2	44.7	60.6	65.8	57.6	8.3
47	Dewana	Shomali	05-30-2006	1345	446.6	234.3	54.2	215.2	482.3	62.4	87.2	89.3	80.3	8.4
54	Alghoai	Deh Sabz	05-21-2006	1145	127.6	77.0	16.5	63.8	164.5	19.7	25.9	30.5	25.4	5.1
59.1	Kata Khel	Eastern Front	05-10-2006	1000	245.2	204.5	47.2	123.0	437.8	56.5	49.8	81.1	72.8	5.3
65	Khair Khana	Central Kabul	05-25-2006	0930	194.6	108.1	21.9	98.2	233.0	26.4	39.8	43.1	34.1	9.0
71	Well 71	Eastern Front	06-05-2007	0940	219.6	157.1	36.1	124.8	378.4	49.8	50.0	70.3	63.8	0.4
72	Shakar dara Qalasad-e-razam	Shomali	06-12-2007	0910	599.6	233.2	61.9	284.7	476.9	69.9	114.1	88.5	89.5	17.4
73	Well 73	Western Front	06-17-2007	1015	232.5	121.8	28.0	101.4	229.2	28.8	40.6	42.5	36.9	8.6
74	Well 74	Shomali	06-19-2007	1140	471.0	279.0	68.6	207.8	529.1	71.5	83.2	98.2	91.5	10.4
104	Dodamast	Western Front	05-13-2006	1100	490.8	250.8	62.2	254.7	555.7	77.2	103.2	102.9	99.4	7.6
105	Karez under Qarga	Paghman and Upper Kabul	05-13-2006	1000	363.7	221.4	47.9	182.4	473.9	57.4	73.9	87.8	73.9	11.4
107	Dashte Karizak	Paghman and Upper Kabul	05-15-2006	1040	191.5	99.5	20.8	98.6	218.6	25.6	39.9	40.5	32.9	6.8
117	Tangi Saedon	Paghman and Upper Kabul	05-15-2006	1220	440.1	252.1	57.3	222.2	543.5	69.1	90.0	100.6	89.0	15.2
129	Kabul Municipality	Central Kabul	05-24-2006	1255	436.5	538.8	42.2	219.1	1,154.5	50.5	88.8	213.8	65.1	15.0
135	Qala-i-Fathulla	Logar	05-17-2006	1050	396.2	221.4	53.1	198.7	473.9	63.6	80.5	87.8	81.9	15.9
153	Parhae Sonati	Central Kabul	05-20-2006	1305	96.3	193.0	23.6	48.2	412.3	28.2	19.5	76.3	36.4	8.0
165	Qala-i-Baqhalak	Central Kabul	05-22-2006	1000	160.1	1,634.1	14.2	80.2	3,494.4	16.9	32.5	647.1	21.8	2.8
168	Shahrak Police	Central Kabul	05-22-2006	1045	1,562.5	889.7	36.1	782.8	1,903.2	43.2	317.2	352.4	55.6	7.8
172	Share Now	Central Kabul	05-22-2006	1145	221.7	454.7	25.0	111.1	973.1	30.0	45.0	180.2	38.6	12.3
182	Qala Wazir	Paghman and Upper Kabul	06-02-2007	1155	505.8	245.9	60.7	239.3	501.2	68.2	95.9	93.0	87.3	11.5
183	Hoot Khel	Central Kabul	06-04-2007	0905	166.8	8,879.6	27.7	76.7	17,572.0	30.2	30.7	3,262.0	38.6	12.4
184	Dehmazang Pampstion well	Paghman and Upper Kabul	06-06-2007	0920	519.7	1,076.9	30.3	299.9	2,609.1	42.2	120.1	484.3	54.1	10.9

Table 13-1. Chlorofluorocarbon and tritium data collected in the Kabul Basin, Afghanistan.—Continued

[CFC, Chlorofluorocarbon; CFC-11, trichlorofluoromethane; CFC-12, dichlorodifluoromethane; CFC-113, trichlorotrifluoroethane; pg kg⁻¹, picograms per kilogram; ppt, parts per trillion; TU, Tritium Unit; nd, not determined]

Site number	Name	Groundwater region	Sample date	Sample time	CFC-11 mass fraction ¹ , pg/kg	CFC-113 mass fraction ¹ , pg/kg	CFC-12 mass fraction ¹ , pg/kg	CFC-11 volume fraction ¹ , ppt	CFC-113 volume fraction ¹ , ppt	CFC-12 volume fraction ¹ , ppt	CFC-11 fraction ² , modern	CFC-113 fraction ² , modern	CFC-12 fraction ² , modern	Tritium, in TU
Groundwater—Continued														
185	Karte New	Central Kabul	06-16-2007	1056	269.6	161.2	34.4	135.4	41.2	345.7	54.2	64.2	52.8	2.0
186	Khair Khana	Central Kabul	06-18-2007	0940	208.9	108.6	25.1	129.0	37.9	281.0	51.7	52.2	48.5	0.6
187	Charakh Aab Pum Azizi Hootak	Logar	06-20-2007	1030	264.6	219.1	50.0	96.8	42.4	354.0	38.8	65.7	54.3	8.5
203	Logar	Logar	05-20-2006	1110	378.6	209.6	49.8	189.6	59.6	448.1	76.8	83.0	76.7	12.0
208	Microtrayan	Central Kabul	05-20-2006	0930	380.4	241.2	44.0	190.6	52.7	516.0	77.2	95.5	67.9	12.3
213	Alluddin	Paghman and Upper Kabul	05-15-2006	1305	545.0	411.6	61.2	273.7	73.4	882.5	1,10.9	163.4	94.5	14.1
219	Khair Khana part 2	Central Kabul	05-24-2006	0935	159.5	105.9	19.8	80.1	23.8	227.2	32.5	42.1	30.6	2.6
221	Bagrami Well 221	Logar	02-19-2007	1120	223.8	149.6	22.9	110.5	27.0	316.1	44.8	58.5	34.7	6.8
223	US Embassy cafe well	Central Kabul	02-22-2007	1400	130.0	158.1	12.2	64.4	14.3	333.5	26.1	61.8	18.5	7.0
	Average				343.6	542.5	38.0	170.9	44.8	1,123.4	69.0	208.3	57.6	9.4
	Standard Deviation				252.9	1,483.7	16.2	127.1	18.4	2,944.3	51.4	546.6	23.6	5.1
	Median				264.6	218.7	36.1	129.0	42.4	448.1	51.7	83.0	54.3	8.6
	Maximum				1,562.5	8,879.6	68.6	782.8	77.2	17,572.0	317.2	3,262.0	99.4	20.1
	Minimum				96.3	77.0	12.2	48.2	14.3	164.5	19.5	30.5	18.5	0.4
Springs														
66.1	Deh Sabz Khaas Spring	Eastern Front	05-16-2006	1110	322.0	232.5	41.7	161.4	50.0	497.7	65.4	92.2	64.4	12.7
67.1	Istefef Spring	Shomali	05-23-2006	1145	382.9	247.5	48.5	192.0	58.1	530.0	77.8	98.1	74.8	18.0
68.1	Gaza Spring	Shomali	05-21-2006	1000	473.0	225.0	59.5	237.2	71.3	481.8	96.1	89.2	91.9	16.3
101	Chandal Bat Spring	Western Front	05-13-2006	1130	751.9	360.2	67.9	377.0	81.3	771.3	152.8	142.8	104.7	11.0
180	Khaja Safa Spring	Central Kabul	06-17-2006	0945	4.9	67.2	2.4	2.5	2.9	143.9	1.0	26.6	3.7	18.0
181	Chara Sib Spring	Logar	06-17-2006	1135	407.0	252.6	57.7	204.1	69.1	540.9	82.7	100.2	89.0	12.5
	Average				390.3	230.9	46.3	195.7	55.4	494.3	79.3	91.5	71.4	14.8
	Standard Deviation				241.3	94.1	23.3	121.0	27.9	201.5	49.0	37.3	36.0	3.1
	Median				394.9	240.0	53.1	198.0	63.6	513.9	80.2	95.1	81.9	14.5
	Maximum				751.9	360.2	67.9	377.0	81.3	771.3	152.8	142.8	104.7	18.0
	Minimum				4.9	67.2	2.4	2.5	2.9	143.9	1.0	26.6	3.7	11.0

Table 13-1. Chlorofluorocarbon and tritium data collected in the Kabul Basin, Afghanistan.—Continued

[CFC, Chlorofluorocarbon; CFC-11, trichlorofluoromethane; CFC-12, dichlorodifluoromethane; CFC-113, trichlorotrifluoroethane; pg kg⁻¹, picograms per kilogram; ppt, parts per trillion; TU, Tritium Unit; nd, not determined]

Site number	Name	Groundwater region	Sample date	Sample time	CFC-11 mass fraction ¹ , pg/kg	CFC-12 mass fraction ¹ , pg/kg	CFC-113 mass fraction ¹ , pg/kg	CFC-11 volume fraction ¹ , ppt	CFC-12 volume fraction ¹ , ppt	CFC-113 volume fraction ¹ , ppt	CFC-11 fraction modern ²	CFC-12 fraction modern ²	CFC-113 fraction modern ²	Tritium, in TU
301	Istalef River	Shomali	2-13-2007	1145	637.7	326.2	89.1	242.7	551.3	79.4	98.4	102.1	102.3	7.8
302	Panjshir River at Sayad	Shomali	02-06-2007	1130	504.7	250.1	64.0	227.9	490.2	69.1	92.4	90.8	89.0	11.2
303	Barak Ab River	Shomali	02-20-2007	1020	494.2	269.9	67.0	218.5	519.1	70.7	88.6	96.1	91.0	8.6
321	Logar River	Logar	02-07-2007	1100	622.8	332.6	84.5	228.0	542.7	72.3	92.4	100.5	93.1	6.5
322	Kabul River at Tangi Gharu	Central Kabul	02-07-2007	1300	700.6	319.2	82.0	285.3	572.7	78.8	115.6	106.0	101.4	7.2
323	Paghman River at Paghman	Paghman and Upper Kabul	02-10-2007	1350	688.9	331.1	92.6	247.6	534.7	77.2	100.3	99.0	99.4	7.2
324	Kabul River at Tang-i Saitdan	Paghman and Upper Kabul	02-10-2007	1100	656.5	326.7	90.2	236.3	525.5	75.6	95.7	97.3	97.4	10.8
301	Istalef River at Istalef	Shomali	06-14-2007	0920	1,090.0	255.7	72.2	611.7	611.6	98.6	245.1	113.5	126.3	nd
301	Istalef River at Istalef	Shomali	07-15-2007	1000	398.0	201.9	51.0	260.5	554.3	82.5	104.4	102.9	105.6	nd
302	Panjshir River at Sayad	Shomali	06-19-2007	1030	531.8	270.3	71.3	285.7	618.7	93.2	114.5	114.9	119.4	nd
321	Logar River	Logar	06-20-2007	1130	238.5	162.4	32.4	190.6	533.3	65.5	76.4	99.0	83.9	nd
322	Kabul River at Tangi Gharu	Central Kabul	06-04-2007	1115	78.9	178.3	40.0	63.9	592.6	82.2	25.6	110.0	105.2	nd
322	Kabul River at Tangi Gharu	Central Kabul	07-04-2007	0955	363.5	165.6	39.1	298.5	556.9	81.4	119.6	103.4	104.3	nd
323	Paghman River at Paghman	Paghman and Upper Kabul	06-02-2007	1030	399.0	208.0	52.3	250.4	553.3	80.3	100.3	102.7	102.8	nd
Average														
Standard Deviation														
Median														
Maximum														
Minimum														

Table 13-1. Chlorofluorocarbon and tritium data collected in the Kabul Basin, Afghanistan.—Continued

[CFC, Chlorofluorocarbon; CFC-11, trichlorofluoromethane; CFC-12, dichlorodifluoromethane; CFC-113, trichlorotrifluoroethane; pg kg⁻¹, picograms per kilogram; ppt, parts per trillion; TU, Tritium Unit; nd, not determined]

Site number	Name	Groundwater region	Sample date	Sample time	CFC-11 mass fraction ¹ , pg/kg	CFC-12 mass fraction ¹ , pg/kg	CFC-113 mass fraction ¹ , pg/kg	CFC-11 volume fraction ¹ , ppt	CFC-12 volume fraction ¹ , ppt	CFC-113 volume fraction ¹ , ppt	CFC-11 fraction ² , modern	CFC-12 fraction ² , modern	CFC-113 fraction ² , modern	Tritium, in TU
181	Chara Sib Spring		12-10-2006	—	—	—	—	281.2	610.1	137.9	112.7	113.3	176.6	—
181	Chara Sib Spring		01-10-2007	—	—	—	—	253.6	542.7	81.4	101.6	100.7	104.2	—
181	Chara Sib Spring		05-29-2007	—	—	—	—	272.1	550.9	94.9	109.0	102.3	121.5	—
181	Chara Sib Spring		06-20-2007	—	—	—	—	494.1	685.0	266.1	197.9	127.2	340.7	—
	Dihsabz-Khas Village		06-03-2007	—	—	—	—	293.5	563.3	108.3	117.6	104.6	138.6	—
	Shomaly Istalef District		06-14-2007	—	—	—	—	418.6	630.4	194.1	167.7	117.0	248.6	—
	Average							335.5	597.1	147.1	134.4	110.8	188.4	
	Standard Deviation							97.5	55.2	70.7	39.0	10.2	90.5	
	Median							287.4	586.7	123.1	115.1	108.9	157.6	
	Maximum							494.1	685.0	266.1	197.9	127.2	340.7	
	Minimum							253.6	542.7	81.4	101.6	100.7	104.2	

¹ Calculated using altitude, recharge temperatures and excess air from Table 13-2.

² Assumes CFC-11, CFC-12, and CFC-113 volume fractions in Kabul Basin air in 2006 of 249.6, 538.7, and 78.1 ppt, respectively, based on North American Air (IAEA, 2006).

Several processes may affect the concentrations and interpretation of CFCs and tritium in the Kabul Basin waters. CFCs can degrade microbially in low-oxygen waters. The relative rates of degradation are in the order CFC-11 >> CFC-113 > CFC-12 (International Atomic Energy Agency, 2006). Consequently, in some low-oxygen samples, there can be an old bias in apparent ages based on CFC-11, whereas apparent ages based on CFC-113 and CFC-12 will be in relatively close agreement. In some cases, there can be other (anthropogenic) sources of CFCs, in addition to that of the atmosphere, such as from some industrial wastewaters (International Atomic Energy Agency, 2006). In this case, water samples may have CFC concentrations greater than that from an atmospheric source, giving a young, or impossibly young, bias.

Mixing relations among the CFC and tritium tracers were examined using tracer-tracer plots. In constructing these plots, it was necessary to assume a recharge temperature and recharge altitude for each water sample in order to calculate CFC volume fractions. For these calculations, the reported sample land-surface altitude was used, or if not available, the median altitude of 1,800 m was used. The recharge temperature determined from measurements of the mass concentrations of nitrogen (N_2) and argon (Ar) dissolved in 16 samples (table 13-2) averaged $12.7 \pm 2.5^\circ\text{C}$; the range was 7.0 to 16.7°C . For CFC-age interpretation, the measured recharge temperature was used if determined; otherwise, the average value was used. Procedures used in evaluating the dissolved-gas compositions are given in Plummer and others (2003) and International Atomic Energy Agency (2006). Most of the water samples analyzed for N_2 and Ar appear to be under somewhat reducing conditions, undergoing denitrification (table 13-2), with as much as 7 mg/L of excess N derived from denitrification of nitrate. However, of the overall data set, including many groundwater samples not analyzed for CFCs, dissolved oxygen mass concentrations averaged 4 to 9 mg/L. Quantities of excess air are estimated to average about 1.1 cc STP per kg. A small correction was applied for the excess air in CFC-age interpretation (International Atomic Energy Agency, 2006).

Atmospheric Input Functions of CFCs and Tritium for the Kabul Basin

In constructing the tracer-tracer plots, atmospheric input functions of CFCs and tritium in precipitation were used to define piston-flow relations (fig. 13-1).

CFCs

The CFC atmospheric input functions were taken as that of North American Air (International Atomic Energy Agency, 2006). Because the CFCs are relatively well-mixed in the Northern Hemisphere in areas remote from urban and industrial centers, this assumption is reasonable and supported by some of the CFC analyses of air from the Kabul Basin (table 13-1). Other samples show an excess of CFCs in Kabul

Basin air today. Modern North American air (International Atomic Energy Agency, 2006) has CFC-11, CFC-12, and CFC-113 volume fractions of approximately 250, 539, and 78 ppt. The median CFC-11, CFC-12, and CFC-113 volume fractions in the six Kabul Basin air samples, expressed as a ratio of modern, are 115, 109, and 158 percent, respectively. Today, there appears to be an excess of CFC-113 in local air of the Kabul Basin, though the source is not known. To a lesser extent, there also is an excess of CFC-11 and CFC-12 relative to North American air in the air samples collected from the Kabul Basin (table 13-1).

Tritium

In constructing the “tritium in precipitation” input function for the Kabul Basin, the available GNIP tritium data for Kabul (International Atomic Energy Agency/WMO, 2004) were examined and compared to the IAEA records from Ottawa and Vienna. Correlations were constructed to help fill in gaps in the Kabul record. As has been noted in the past, the Ottawa record contains input from a local tritium source in post-1980 precipitation. The available Kabul tritium data are nearly identical to the Vienna record in the past 20+ years. The “tritium in precipitation” input function used for the Kabul Basin was constructed from a correlation with Ottawa data prior to the early 1960s, uses observed Kabul data where available, uses a correlation with the Vienna record where Kabul data are missing in the post-1960s to mid-1970s, and uses the Vienna record directly in recent years where Kabul data are missing.

CFCs in Groundwater

Among the 41 groundwater samples from wells and springs analyzed for CFCs, the median volume fractions of CFC-11, CFC-12, and CFC-113, expressed as a ratio to that in modern North American air, were 72, 86, and 65 percent, respectively. Six samples had CFC-11 amounts that exceeded equilibrium with modern air; 11 samples had CFC-12 amounts that exceeded equilibrium with modern air values, and one of the CFC-113 values in groundwater exceeded equilibrium with modern air. Excesses of CFC-11 and CFC-12 greater than those of modern air-water equilibrium co-occurred in five of the six samples with CFC-11 amounts being greater than equilibrium with modern air (table 13-1). For the samples that had volume fractions that exceeded those of modern values, the median excesses were factors of 1.2 for CFC-11 and 1.8 for CFC-12 relative to waters in equilibrium with modern air. Of the three CFCs measured, CFC-12 had a higher frequency to exceed air-water equilibrium than did CFC-11 or CFC-113. Only one of the six spring samples had excess CFCs (water from site 101) where the volume fractions of all three CFCs were somewhat elevated above that for modern air-water equilibrium. The median CFC-11, CFC-12, and CFC-113 volume fractions in water from springs were 80, 95, and 82 percent modern, respectively.

CFCs in Surface Water and Air

The median volume fractions of CFC-11, CFC-12, and CFC-113 in the 14 surface-water samples (table 13-1), correcting for altitude and water temperature, were 99, 102, and 102 percent modern, respectively. Apparently, today the local surface waters are near equilibrium with the modern atmosphere, but in the past, there may have been local inputs of CFC-12 (and CFC-11) that exceeded North American air concentrations resulting in enrichment with respect to CFC-12 (and to a lesser extent, CFC-11) in some of the older waters. Alternatively, other land-use activities may have introduced an excess of CFC-12 (and CFC-11) in the past; an activity that is currently limited. Excess of all three CFCs were measured in all six air samples collected in remote regions of the Kabul Basin (table 13-1).

CFC Ages

Two processes have affected CFC-age interpretation in Kabul Basin groundwater: (1) excess CFC sources, in addition to that of the atmosphere in the Kabul region, resulting in CFC excesses in some surface water, and (2) degradation of CFCs, primarily CFC-11. The extent to which any one sample has been affected by one or both of these processes is variable. Evidence of contamination and degradation processes is seen in plots comparing CFC volume fractions in water and air with model calculations (fig. 13-2).

Volume fractions of CFC-11 and CFC-113 are compared in figure 13-2A. Many of the CFC-11 and CFC-113 volume fractions plot along the binary dilution line as if modern water were diluted with old, CFC-free water. Accordingly, seven samples contain an excess of CFC-113 (fig. 13-2A). Alternatively, the CFC-11 volume fractions may be biased low because of microbial degradation. In this case, the CFC-113 values may be in the normal range. Similar interpretation based on CFC-11 and CFC-113 values apply to the surface-water samples, which are either diluted with old, CFC-free water or degraded.

Either most of the samples contain an excess of CFC-12 or most are degraded with regard to CFC-11 (fig. 13-2B). Most of the groundwater samples have CFC-12 and CFC-113 concentrations that plot within the envelope of "normal" values, bounded by model lines of piston flow and binary mixing (fig. 13-2C). Many samples indicate mixtures, and others plot near the piston-flow line (unmixed samples) (fig. 13-2C). Still other samples (groundwater, surface water, and water from springs) plot approximately parallel to results for piston flow but are either degraded in CFC-113 or elevated in CFC-12 (fig. 13-2C). Several lines of evidence point to microbial degradation: (1) most of the samples analyzed for dissolved N_2 and Ar apparently have low dissolved oxygen concentration and have undergone denitrification (table 13-2), though it cannot be determined to what extent the samples were degraded on storage in Afghanistan and during shipment

to the Reston Chlorofluorocarbon Laboratory of the U.S. Geological Survey; (2) one sample contains dissolved methane (table 13-2); (3) several surface-water samples are degraded in CFCs, particularly CFC-11 (table 13-2). Still other surface-water and groundwater samples are elevated in CFC-12, so it is likely that both processes have affected some of the samples to varying extents.

The piston-flow ages that could be calculated from the CFC groundwater data are summarized in table 13-3. The median piston-flow ages for CFC-11, CFC-12, and CFC-113 from data from the 34 wells were 31, 24, and 22 years, respectively, with ranges of piston-flow ages of 13 to 38, 9 to 35, and 16 to 31 years, respectively. Dual ages could only be calculated for three samples (wells 13, 104, and 213). All other samples have CFC piston-flow ages older than the turnover in atmospheric CFC input functions (fig. 13-1). These preliminary results suggest little modern water was sampled. Most of the samples either pre-date the turnover in CFC air curves or are dilutions of young water.

Seventeen of the samples had CFC concentrations in the range that permitted evaluation as binary mixtures of young and old water, based on CFC-113 and CFC-12. For these, the average age of the young part was 21 ± 2 years and the fraction of that young water averaged 76 ± 18 percent. Using the ratio of the CFC-113 and CFC-11 volume fractions, the age of the young fraction in 24 samples averaged 16 ± 3 years with a young fraction of 58 ± 22 percent. In both cases, relatively high fractions of young water were indicated with ages of 16 to 21 years.

Age Variations Between Groundwaters

The differences in the average piston-flow ages, the average ratio-based ages, average fraction of young water in mixtures, average fraction of modern water, and average tritium concentration in groundwater from each of the seven sub-regions of the Kabul Basin are relatively small (table 13-4) and similar to the average values for the Kabul Basin. The most reliable ages are judged to be the CFC-12 and CFC-113 piston-flow ages and ratio-based ages determined from the ratios of the CFC-113 and CFC-12 volume-fraction data. The average CFC-12 piston-flow ages ranged from 20 years (Paghman and Upper Kabul subbasin) to 28 years (Deh Sabz and Central Kabul subbasin), and based on CFC-113 range from 19 years (Shomali subbasin) to 26 years (Central Kabul subbasin) (table 13-4). The ratio-based ages are slightly younger than the piston-flow ages and ranged from 15 years (Shomali subbasin) to 23 years (Western Front Source Area) on the basis of the CFC-113/CFC-12 ratio of volume fractions. The percent of young water in those samples modeled as mixtures of young and tracer-free water tends to decrease with depth below the water table; average values ranged from 55 percent (Paghman and Upper Kabul subbasin) to 95 percent (Eastern Front Source Area) (table 13-4). However, the similarity in piston-flow and ratio-based ages supports the conclusion that most of the waters are unmixed, i.e., they

are, for the most part, not dilutions of a young fraction. In this case, the piston-flow ages or ages based on the exponential model most likely apply.

Water pumped from relatively large open intervals in alluvial basin-fill sediment may be interpreted best using exponential mixing models. In this case, mean ages derived from the exponential model will be greater than the

piston-flow ages in samples where the piston-flow ages are greater than about 10–15 years, as in the present samples. As a guide, selected values of mean exponential age are shown along the exponential model lines in figures 13-2A-C. The exponential-model mean ages appear to range from about 5 to 100 years, but again do not differ greatly between groundwater subbasins and source area (fig. 13-2).

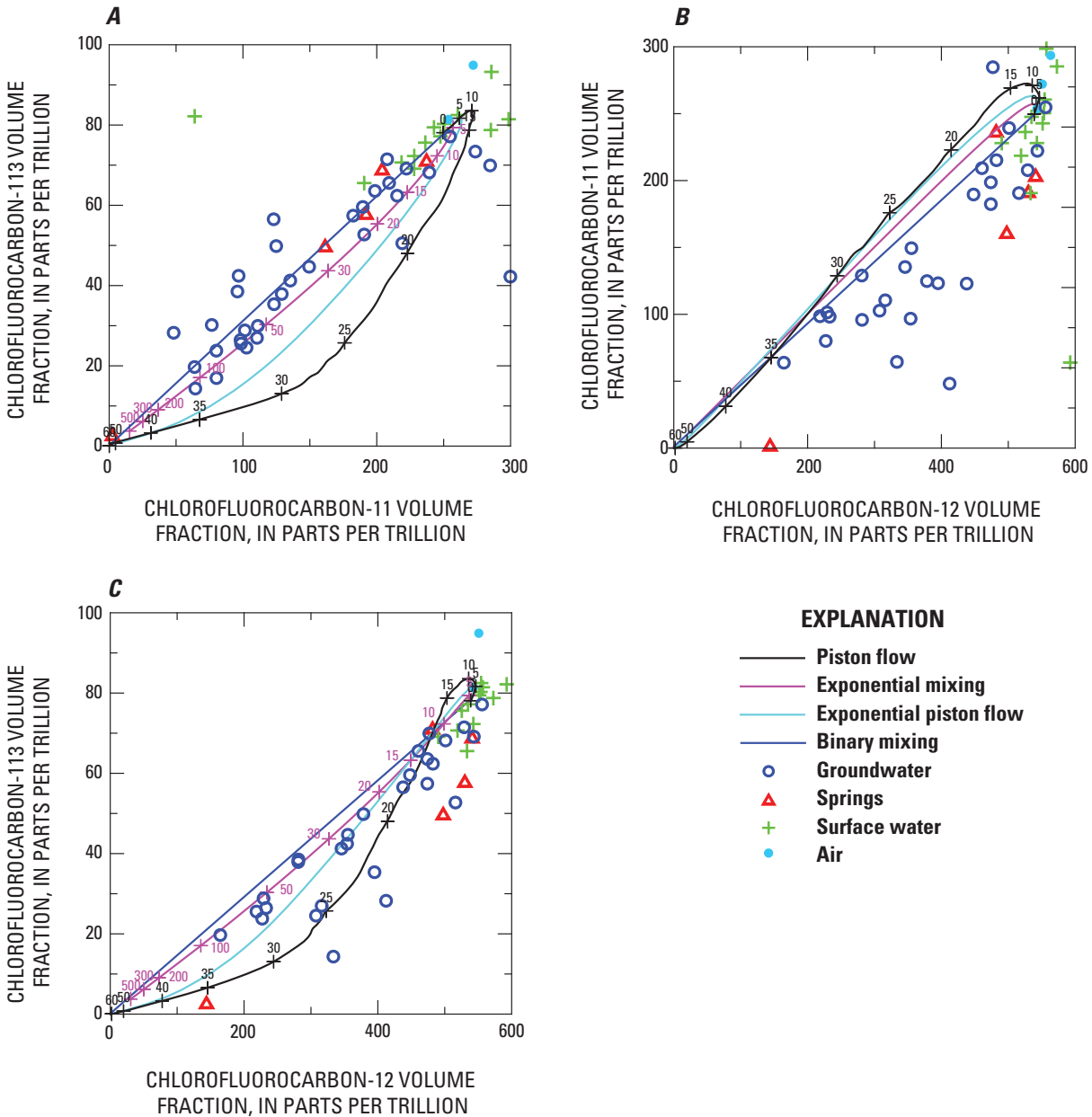


Figure 13-2. Tracer-Tracer plots comparing volume fractions of CFCs in groundwater, water from springs, surface water, and air in the Kabul Basin. The black line represents piston flow, corresponding to CFC volume fractions in parts per trillion (ppt) in North American air. The blue line represents binary mixing of modern water and old, tracer-free water. Model results for the exponential mixing model (magenta) and exponential-piston model (cyan) also are shown (A) CFC-113 versus CFC-11; (B) CFC-11 versus CFC-12; and (C) CFC-113 versus CFC-12. Selected piston flow ages, in years, are given on the piston-flow lines in A–C, and for the exponential model in A and C.

Table 13-2. Summary of dissolved gas composition of selected groundwater samples, estimated excess N_2 from denitrification, estimated recharge temperature and estimated quantity of excess air in the Kabul Basin, Afghanistan.

[m, meters; °C, degrees Celsius; mg/L, milligrams per liter; cc, cubic centimeter; STP/L, Standard Temperature and Pressure per liter]

Site number	Name	Sample date	Time	Estimated recharge altitude (m)	Water temperature (°C)	N_2 (mg/L)	Ar (mg/L)	O_2 (mg/L)	CO_2 (mg/L)	CH_4 (mg/L)	Estimated excess N_2 from denitrification (mg/L)	Calculated recharge temperature (°C)	Calculated excess air cc STP/L
33	Well 033	05/15/07	1000	1,892	nd	16.46	0.5592	0.17	24.52	0.0000	1.0	10.6	1.3
54	Well 054	05/08/07	1000	1,783	nd	13.83	0.4810	1.91	14.73	0.0000	1.0	16.0	0.0
71	Well-71	06/05/07	0940	1,791	20.0	19.28	0.5794	0.14	22.13	0.0000	1.0	15.1	0.4
72	Well-72	06/12/07	0910	1,873	15.2	15.81	0.5425	0.13	23.55	0.0000	1.0	11.5	0.9
73	Well-73	06/17/07	1015	1,593	16.3	17.77	0.5845	0.15	11.48	0.0000	1.5	10.6	1.5
74	Well-74	06/19/07	1140	1,659	15.2	16.07	0.5755	0.32	38.46	0.0000	0.0	11.0	1.6
104	Well 104 Dodumust	05/02/07	1000	2,080	13.5	14.40	0.4886	0.15	22.12	0.0000	1.0	15.0	0.8
129	Well 129	05/19/07	1120	1,807	16.1	16.04	0.5417	0.13	38.59	0.0000	1.0	12.5	1.3
165	Well 165	05/14/07	0930	1,788	15.8	15.70	0.5271	0.14	23.48	0.0000	1.0	13.9	1.3
182	Qala Wazir Well-182	06/02/07	1155	1,933	16.0	17.42	0.5439	0.14	30.01	0.0000	2.5	11.3	1.0
183	Hoot khel Well-183	06/04/07	0905	1,795	18.8	17.99	0.5600	0.14	17.89	0.0083	2.5	11.1	1.3
184	Dehmazang Pampstion Well-184	06/06/07	0920	1,811	15.6	21.12	0.5070	0.11	38.11	0.0000	7.0	15.4	1.2
185	Karte New Well-185	06/16/07	1056	1,810	20.3	15.22	0.4600	0.12	17.17	0.0000	nd ¹	nd ¹	nd ¹
186	Khair Khana Well-186	06/18/07	0940	1,817	18.5	18.28	0.4853	0.12	7.62	0.0000	5.0	16.7	0.6
187	Charkh Aab pum Azizi Hootak Well-187	06/20/07	1030	1,825	15.4	19.95	0.6154	0.14	32.14	0.0000	3.0	7.0	1.4
221	Bagrami Well 221	02/19/07	1120	1,797	13.8	15.78	0.5384	0.33	22.15	0.0000	1.0	12.4	1.0
223	US Embassy Cafe Well	02/22/07	1400	1,798	16.3	16.88	0.5479	0.17	23.61	0.0000	1.5	12.5	1.6

¹ Sample may be degassed.

Table 13-3. Summary of piston-flow and binary mixing model ages of groundwater and spring water based on chlorofluorocarbon data in the Kabul Basin, Afghanistan.

[CFC, chlorofluorocarbon; CFC-11, trichlorofluoromethane; CFC-12, dichlorodifluoromethane; CFC-113, trichlorotrifluoroethane; 1, calculated on rising limb of CFC air curve; 2, calculated on falling limb of CFC air curve; PF, piston-flow model age; Ratio Age, age based on CFC ratio; NP, not possible; nd, not determined; Contam., contaminated--exceeds concentration in water in equilibrium with modern air; Modern, approximately zero age]

Site number	Name	Groundwater region	Sample date	Sample time	CFC-11 PF age (1) years ¹	CFC-11 PF age (2) years ¹	CFC-12 PF age (1) years ¹	CFC-12 PF age (2) years ¹	CFC-113 PF age (1) years ¹	CFC-113 PF age (2) years ¹	CFC-113/ CFC-12 ratio age years ¹	Percent young water in mixture calculated from CFC-113 ¹	CFC-113/ CFC-11 ratio age years ¹	Percent young water in mixture calculated from CFC-113 ¹
13	Pacha Sahab	Deh Sabz	05-16-2006	1200	31.0	NP	20.5	0.4	23.0	NP	21.4	82.6	16.0	75.9
28	Obehakan Ball	Shomali	05-23-2006	1300	21.9	NP	34.4	NP	18.1	NP	7.9	87.2	11.7	83.5
33	Mir Afghan	Western Front	05-23-2006	1030	32.6	NP	26.9	NP	26.1	NP	25.6	98.3	19.1	56.2
37	Shekhu	Deh Sabz	05-14-2006	1000	33.0	NP	28.7	NP	22.4	NP	18.2	61.8	NP	NP
42	Godar	Shomali	05-28-2006	0810	28.7	NP	24.2	NP	21.4	NP	19.4	82.4	14.4	80.7
47	Dewana	Shomali	05-30-2006	1345	21.4	NP	17.4	NP	18.4	NP	NP	NP	15.9	76.6
54	Alghoi	Deh Sabz	05-21-2006	1145	36.1	NP	34.6	NP	27.6	NP	20.1	39.8	11.1	83.6
59.1	Kata Khel	Eastern Front	05-10-2006	1000	30.9	NP	19.6	NP	19.4	NP	18.9	98.3	NP	NP
65	Khair Khana	Central Kabul	05-25-2006	0930	32.9	NP	31.1	NP	25.4	NP	20.9	58.7	17.4	68.2
71	Well 71	Eastern Front	06-05-2007	0940	32.2	NP	23.7	NP	21.4	NP	19.9	86.4	NP	NP
72	Shakar dara Qalasad-e-razam	Shomali	06-12-2007	0910	Modern	Contam.	18.7	NP	18.4	NP	NP	NP	NP	NP
73	Well 73	Western Front	06-1720-07	1015	33.7	NP	32.5	NP	25.7	NP	20.7	54.8	17.5	74.1
74	Well 74	Shomali	06-19-2007	1140	23.2	NP	18.0	NP	18.2	NP	NP	NP	NP	NP
104	Dodamast	Western Front	05-13-2006	1100	17.9	2.1	8.9	1.9	16.1	NP	NP	NP	13.6	81.7
105	Karez under Qarga	Paghman/Upper Kabul	05-13-2006	1000	25.0	NP	17.9	NP	19.2	NP	NP	NP	10.9	83.7
107	Dashte Karizak	Paghman/Upper Kabul	05-15-2006	1040	32.9	NP	31.9	NP	25.6	NP	20.6	54.9	17.9	64.9
117	Tangi Saidan	Paghman/Upper Kabul	05-15-2006	1220	20.9	NP	14.4	Contam.	17.4	NP	NP	NP	10.9	83.7
129	Kabul Municipality	Central Kabul	05-24-2006	1255	20.9	NP	Contam.	Contam.	20.1	NP	NP	NP	18.4	61.2
135	Qala-i-Fathulla	Logar	05-17-2006	1050	23.0	NP	17.7	NP	18.2	NP	NP	NP	10.9	83.7
153	Parkhae Sonati	Central Kabul	05-20-2006	1305	37.9	NP	20.9	NP	24.9	NP	NP	NP	NP	NP
165	Qala-i-Baqhalak	Central Kabul	05-22-2006	1000	34.4	NP	Contam.	Contam.	28.7	NP	NP	NP	20.9	45.2
168	Shabrak Police	Central Kabul	05-22-2006	1045	Contam.	Contam.	Contam.	Contam.	21.4	NP	NP	NP	NP	NP
172	Share Now	Central Kabul	05-2220-06	1145	31.9	NP	Contam.	Contam.	24.4	NP	NP	NP	17.4	68.2
182	Qala Wazir	Paghman/Upper Kabul	06-02-2007	1155	20.2	-0.6	16.9	NP	18.9	NP	NP	NP	17.4	74.1
183	Hoot Khel	Central Kabul	06-04-2007	0905	35.7	NP	Modern	NP	25.2	NP	NP	NP	NP	NP

Table 13-3. Summary of piston-flow and binary mixing model ages of groundwater and spring water based on chlorofluorocarbon data in the Kabul Basin, Afghanistan.—Continued

[CFC, chlorofluorocarbon; CFC-11, trichlorofluoromethane; CFC-12, dichlorodifluoromethane; CFC-113, trichlorotrifluoroethane; 1, calculated on rising limb of CFC air curve; 2, calculated on falling limb of CFC air curve; PF, piston-flow model age; Ratio Age, age based on CFC ratio; NP, not possible; nd, not determined; Contam., contaminated--exceeds concentration in water in equilibrium with modern air; Modern, approximately zero age]

Site number	Name	Groundwater region	Sample date	Sample time	CFC-11 PF age (1) years ¹	CFC-11 PF age (2) years ¹	CFC-12 PF age (1) years ¹	CFC-12 PF age (2) years ¹	CFC-113 PF age (1) years ¹	CFC-113 PF age (2) years ¹	CFC-113/ CFC-12 ratio age years ¹	Percent young water in mixture calculated from CFC-113 ¹	CFC-113/ CFC-11 ratio age years ¹	Percent young water in mixture calculated from CFC-113 ¹
Groundwater—Continued														
184	Dehmazang Pamp-stion well	Paghman/Upper Kabul	06-06-2007	0920	Contam.	Contam.	Contam.	Contam.	22.7	NP	NP	NP	NP	NP
185	Karte New	Central Kabul	06-16-2007	1056	30.7	NP	25.5	NP	23.0	NP	21.2	83.7	19.0	64.9
186	Khair Khana	Central Kabul	06-18-2007	0940	31.5	NP	30.0	NP	23.5	NP	19.5	61.9	16.5	78.8
187	Charkh Aab Pum Azizi Hootak	Logar	06-20-2007	1030	34.2	NP	25.2	NP	22.7	NP	21.2	85.7	NP	NP
203	Logar	Logar	05-20-2006	1110	23.9	NP	19.4	NP	18.9	NP	18.4	98.0	10.9	83.7
208	Microrayan	Central Kabul	05-20-2006	0930	24.1	NP	14.6	NP	19.9	NP	NP	NP	16.9	71.2
213	Alluddin	Paghman/Upper Kabul	05-15-2006	1305	12.9	11.5	Contam.	Contam.	16.9	NP	NP	NP	NP	NP
219	Khair Khana part 2	Central Kabul	05-24-2006	0935	34.4	NP	31.4	NP	26.4	NP	21.9	59.9	15.1	79.5
221	Bagrami Well 221	Logar	02-19-2007	1120	32.8	NP	27.0	NP	25.8	NP	24.9	92.3	19.5	58.9
223	US Embassy cafe well	Central Kabul	02-22-2007	1400	36.8	NP	26.0	NP	30.8	NP	NP	NP	21.0	49.1
Average					28.7	4.4	23.5	1.1	22.2	nd	20.0	75.7	15.8	72.1
Standard Deviation					6.4	6.4	6.8	1.1	3.7	nd	3.7	18.3	3.3	11.5
Median					31.3	2.1	23.9	1.1	22.4	nd	20.6	82.6	16.7	75.0
Maximum					37.9	11.5	34.6	1.9	30.8	nd	25.6	98.3	21.0	83.7
Minimum					12.9	-0.6	8.9	0.4	16.1	nd	7.9	39.8	10.9	45.2

Table 13-3. Summary of piston-flow and binary mixing model ages of groundwater and spring water based on chlorofluorocarbon data in the Kabul Basin, Afghanistan.—
Continued

[CFC, chlorofluorocarbon; CFC-11, trichlorofluoromethane; CFC-12, dichlorodifluoromethane; CFC-113, trichlorotrifluoroethane; 1, calculated on rising limb of CFC air curve; 2, calculated on falling limb of CFC air curve; PF, piston-flow model age; Ratio Age, age based on CFC ratio; NP, not possible; nd, not determined; Contam., contaminated--exceeds concentration in water in equilibrium with modern air; Modern, approximately zero age]

Site number	Name	Groundwater region	Sample date	Sample time	CFC-11 PF age (1) years ¹	CFC-11 PF age (2) years ¹	CFC-12 PF age (1) years ¹	CFC-12 PF age (2) years ¹	CFC-113 PF age (1) years ¹	CFC-113 PF age (2) years ¹	CFC-113/ CFC-12 ratio age years ¹	CFC-113/ CFC-11 ratio age years ¹	Percent young water in mixture calculated from CFC-113 ¹	Percent young water in mixture calculated from CFC-113 ¹
66.1	Deh Sabz Khaas Spring	Eastern Front	05-16-2006	1110	27.5	NP	19.6	NP	20.4	NP	20.4	11.4	99.9	83.5
67.1	Istalef Spring	Shomali	05-23-2006	1145	23.7	NP	18.6	NP	19.1	19.1	18.4	13.1	92.7	81.2
68.1	Gaza Spring	Shomali	05-21-2006	1000	19.4	NP	17.1	NP	17.1	17.1	NP	14.6	NP	80.9
101	Chandal Bai Spring	Western Front	05-13-2006	1130	Contam.	Contam.	Contam.	Contam.	14.6	4.6	NP	NP	NP	NP
180	Khaja Safa Spring	Central Kabul	06-17-2006	0945	56.1	NP	46.0	NP	45.6	NP	0.0	0.0	NP	NP
181	Chara Sib Spring	Logar	06-17-2006	1135	22.5	NP	15.5	NP	17.6	NP	NP	NP	NP	NP
	Average				29.8	nd	23.4	nd	22.4	4.6	12.9	9.8	96.3	81.9
	Standard Deviaton				15.0	nd	12.7	nd	11.5	nd	11.2	6.6	5.1	1.4
	Median				23.7	nd	18.6	nd	18.3	4.6	18.4	12.2	96.3	81.2
	Maximum				56.1	nd	46.0	nd	45.6	4.6	20.4	14.6	99.9	83.5
	Minimum				19.4	nd	15.5	nd	14.6	4.6	0.0	0.0	92.7	80.9

¹ Calculated using altitude, recharge temperatures and excess air from Table 13-2.

Table 13-4. Summary of average ages, percentages of young water, and percentages of modern water, based on concentrations of chlorofluorocarbons and tritium in groundwater and water from springs by subbasin and source area in the Kabul Basin, Afghanistan.

[Location of basins shown on figure 6. Average CFC values do not include water from Karez 105 (site number 105). CFC, chlorofluorocarbon; CFC-11, trichlorofluoromethane; CFC-12, dichlorodifluoromethane; CFC-113, trichlorotrifluoroethane; TU, Tritium Unit]

Groundwater subbasin or area	Average piston flow ages in years ¹			Average ratio-based ages and percent young water ¹				Average percent modern ²			Tritium in TU
	CFC-11	CFC-12	CFC-113	Age from CFC-113/CFC-12 ratio	Percent young water from CFC-113	Age from CFC-113/CFC-11 ratio	Percent young water from CFC-113	CFC-11	CFC-12	CFC-113	
Eastern Front Source Area	30	21	20	20	95	11	84	55	81	67	6.1
Western Front Source Area	28	23	21	23	77	17	71	85	86	68	12.0
Shomali	23	21	19	15	87	14	81	86	88	81	13.5
Deh Sabz	33	28	24	20	61	16	80	38	52	40	7.6
Central Kabul	34	28	26	17	66	18	65	63	394	39	8.4
Paghman and Upper Kabul	22	20	20	21	55	14	77	89	162	72	12.1
Logar	27	21	21	22	92	14	75	65	79	67	10.4

¹ Averages of all samples that could be dated using CFCs, excluding CFC contaminated samples.

² Average of all samples that could be dated using CFCs, including CFC contaminated samples.

Although the average CFC-based ages are similar throughout the Kabul Basin, there are apparently some age differences on relatively local scales within the Kabul Basin groundwaters. Many of the CFC-11 apparent ages are older than those based on CFC-12 and CFC-113, particularly in parts of the Central Kabul, Deh Sabz, and Shomali regions (figs. 13-3–13-5). The relatively older CFC-11-based ages are likely the result of microbial degradation of CFC-11, which causes an old bias in apparent age. There is a greater tendency for elevated CFC-12, and to a lesser extent, CFC-11, amounts (noted “Contaminated”, meaning volume fractions exceed modern air-water equilibrium values) in the Central Kabul and Paghman and Upper Kabul regions (figs. 13-3, 13-4). The elevated CFC-11 and CFC-12 volume fractions likely reflect localized anthropogenic sources of CFCs in the more urban areas. Some of the CFC-113 apparent ages are younger than those based on CFC-12 in parts of the Shomali, Deh Sabz, and Central Kabul regions. Localized anthropogenic sources of CFC-113 and (or) binary mixing of young and old water would lead to a young bias in CFC-113 apparent ages (fig. 13-5). However, none of the groundwater samples are contaminated (exceed modern air-water equilibrium values) with CFC-113, yet modern air samples from the region are substantially elevated in CFC-113. Apparently, the elevated CFC-113 volume fractions in modern air are a recent phenomenon in the Kabul Basin.

Age Gradients in Groundwater

Well depth and water-level data were available for 25 of the 35 wells sampled for CFCs. However, there was no information on length of well casing or depth of the open interval for any of the wells. Information on variations in groundwater age with depth below the water table was obtained by plotting the CFC apparent (piston-flow) ages as a function of the mid-depth of the saturated interval between the water table and total depth of the well (fig. 13-6). All three tracers show increasing age with depth below the water table. The depth gradients ranged from 1.4 to 2.8 m/year. Assuming a saturated porosity of 25 percent, the age gradients imply a vertical component of recharge of 0.35 to 0.7 m/year. Because most of the groundwater recharge is thought to be from infiltration of water beneath streams and rivers, this range of estimated recharge rate applies primarily to infiltration of surface water beneath irrigation canals, streams, and rivers, rather than spatially across the basin.

It is interesting that the depth-age gradients of figure 13-6 do not appear to extrapolate to zero age at the water table, implying apparent ages of 10 to 15 years at the water table. As pointed out above, only a few samples can be interpreted with dual ages that would yield very young ages. Most of the water samples appear to have piston-flow ages that precede the turnover in atmospheric CFC air curves (early- to mid-1990s). Further, it is unlikely that infiltration from rivers and streams passes through deep unsaturated zones that might exchange CFCs with old resident air. It is more likely that the trends in depth-age gradients turn asymptotically, approaching zero age at the water table; but because of the relatively large open intervals of the wells, insufficient discrete shallow water-table samples were obtained that could demonstrate this trend.

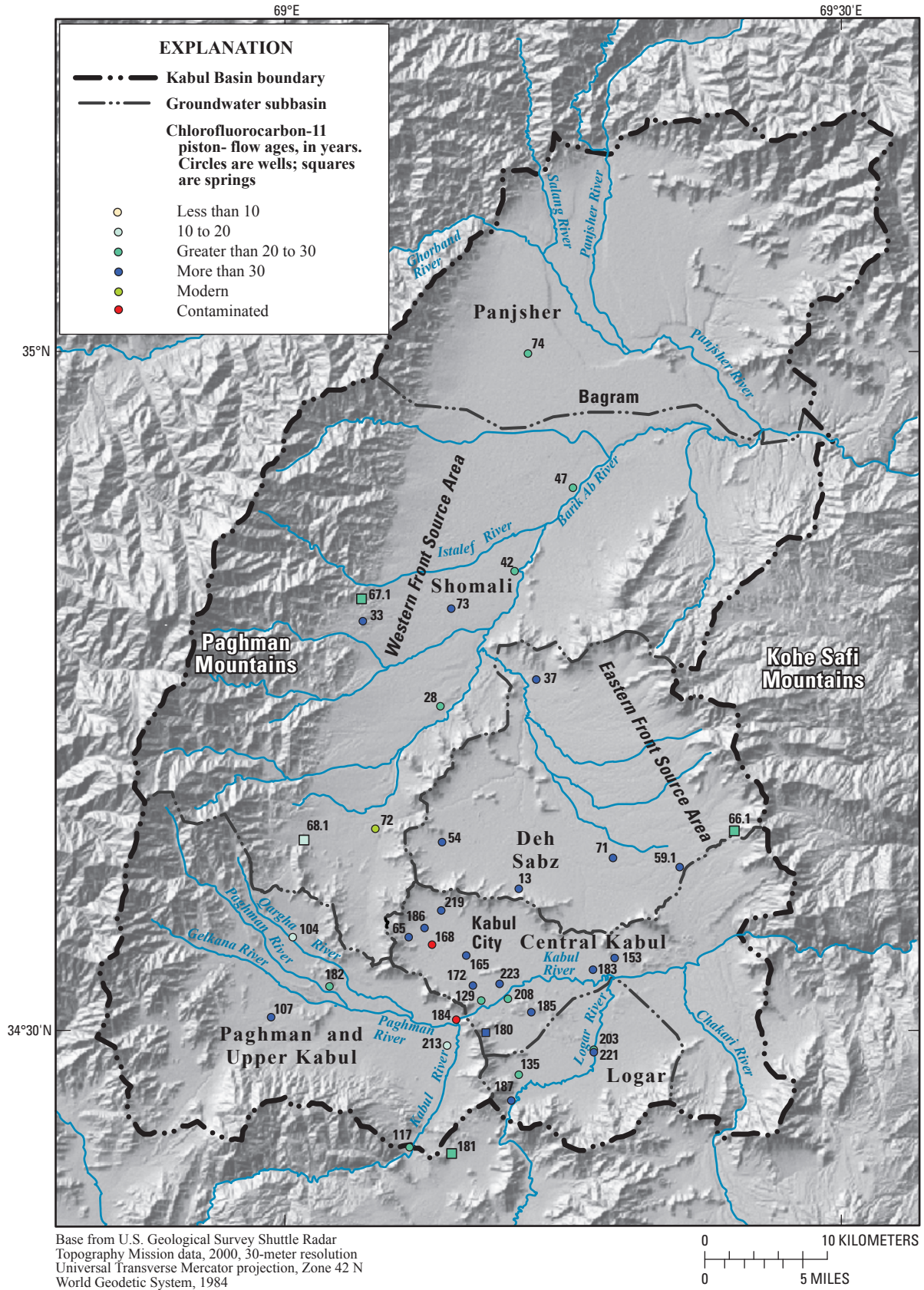
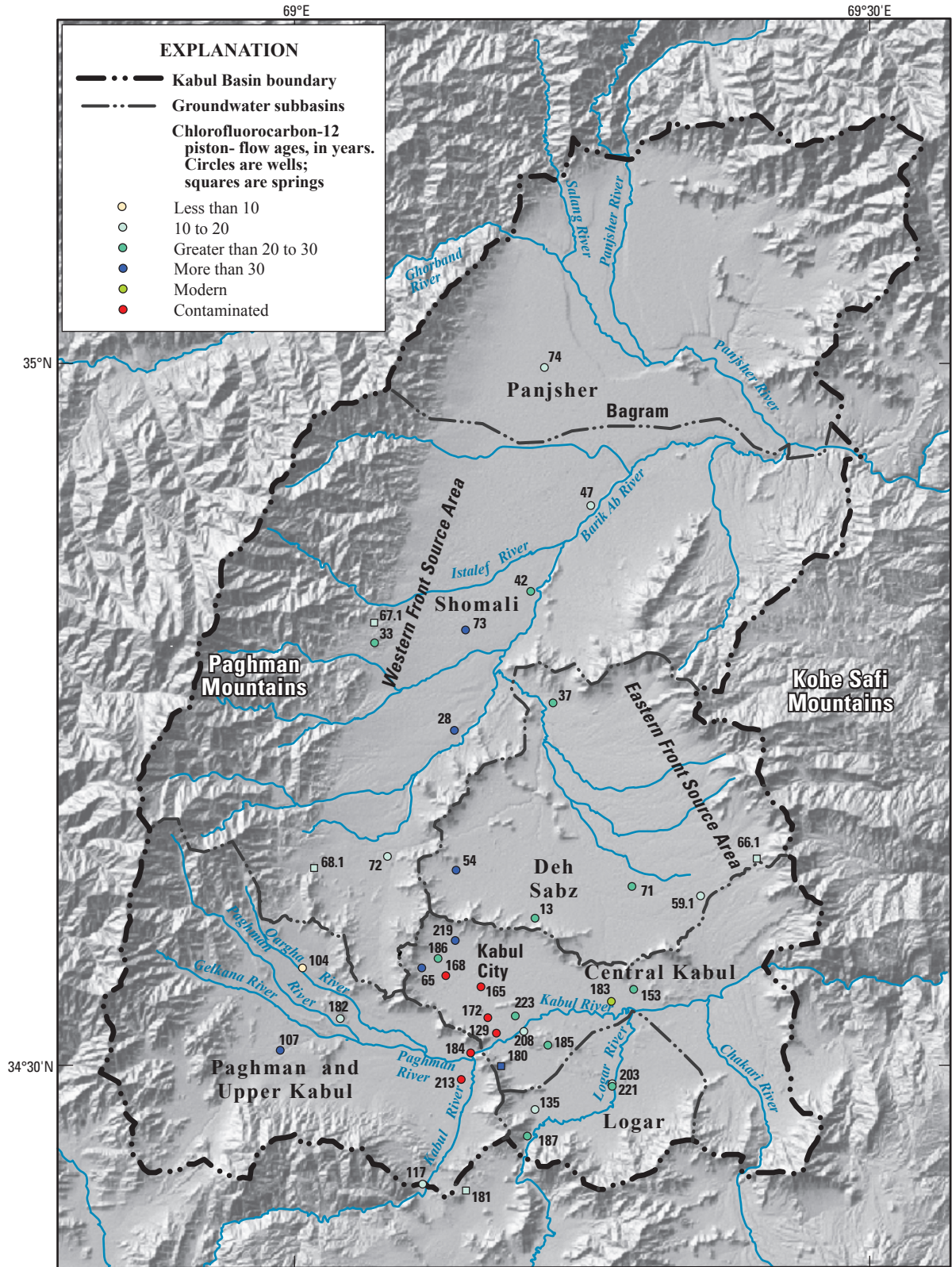


Figure 13-3. CFC-11 piston-flow ages in the Kabul Basin, Afghanistan.



Base from U.S. Geological Survey Shuttle Radar Topography Mission data, 2000, 30-meter resolution Universal Transverse Mercator projection, Zone 42 N World Geodetic System, 1984

Figure 13-4. CFC-12 piston-flow ages in the Kabul Basin, Afghanistan.

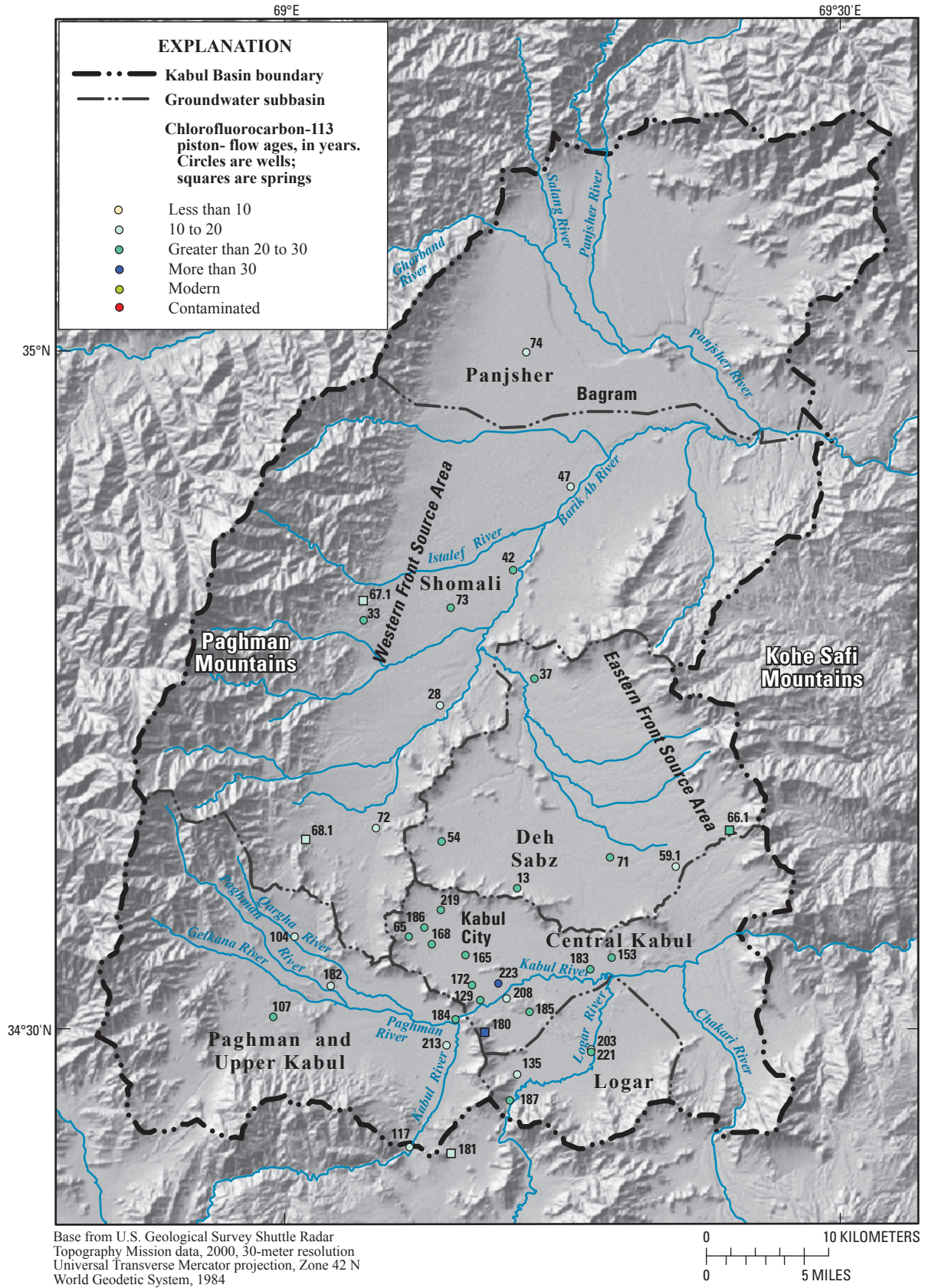


Figure 13-5. CFC-113 piston-flow ages in the Kabul Basin, Afghanistan.

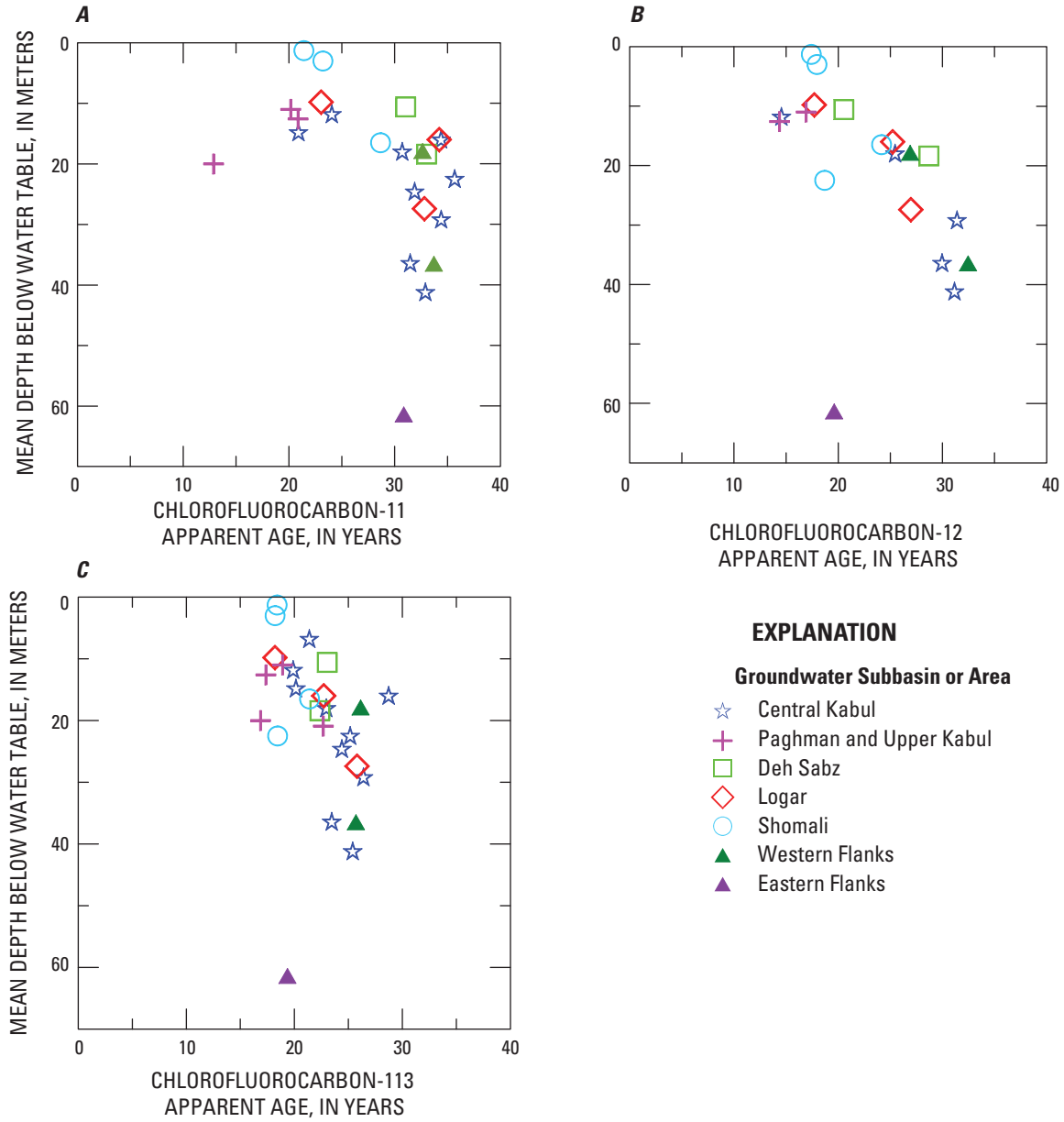


Figure 13-6. Apparent (piston-flow) ages as a function of depth below the water table. Symbols are at the mid-depth of the saturated interval intercepted by the well. The ages were based on (A) CFC-11, (B) CFC-12, and (C) CFC-113. (This figure is the same as figure 25).

Although water would infiltrate nearly vertically beneath the rivers, the water is expected to move laterally away from the rivers to areas of considerably less recharge, resulting in older age near the water table at distances further from rivers and other sources of surface-water infiltration. As a result, the observed depth-age gradients provide only a rough estimate of recharge rate that can be applied only near rivers and streams. Future modeling efforts may be able to utilize the depth-age information to derive more reliable estimates of recharge rates from rivers and streams in the Kabul Basin.

Comparison of CFC and Tritium Data

The CFC transient tracer data are examined in relation to tritium data in figure 13-7. Because of the greatly different shape in input function over time relative to that of CFCs, tritium is a particularly useful environmental tracer in combination with CFC data in interpreting mixing models and groundwater age.

Three categories of samples are apparent in examining tritium in relation to CFCs (fig. 13-7). The first group of samples plot close to the piston-flow line, including both groundwater and surface-water samples. These samples are thought to be mostly unmixed and likely have valid apparent (piston-flow) ages. A second group of samples plot below the piston-flow-model line, and these samples may be dilutions of post-bomb era waters (including modern water) with older water low in tracer concentration. The third group of samples plots above the piston-flow line and includes surface water, groundwater, and water from springs. Some of these samples could be interpreted as exponential or exponential-piston

flow mixtures with mean ages of 5 to nearly 40 years, having somewhat older ages than the apparent (piston-flow) ages. Other samples from this group plot above the exponential and exponential-piston-flow model lines. These samples may represent a group of somewhat older waters recharged in approximately the late 1970s to early 1980s, during a time of elevated CFC concentrations in the Kabul Basin environment. Selected recharge years, marked (in black) along the piston-flow model lines in figure 13-6, can be used to infer tritium-based ages for these samples.

Another possibility to explain the elevated tritium in some samples is to consider a groundwater lag that affects the tritium concentration in groundwater discharge to rivers, because of the mean residence time of groundwater (Michel, 1992). A groundwater lag could shift the bomb-era tritiated water to somewhat younger ages, but probably not the 25–30 years implied by the samples with elevated tritium. Another alternative hypothesis is that some of the Kabul Basin waters were slightly contaminated with tritium in the past 20 years or so, but there is no evidence for this possibility.

Unfortunately, there are not sufficient data to resolve the multiple hypotheses for the origin of the waters plotting above the model lines in figure 13-7. However, data from one spring (site 180) has very low CFC-11 and CFC-113 but elevated tritium and CFC-12. The CFC-11, CFC-113, and tritium data are concordant suggesting that this sample has a mean age from the late 1950s to early 1960s, but it also contains a small fraction of water contaminated in CFC-12 (fig. 13-7). This observation supports the hypothesis that the waters plotting above the model lines have elevated CFC concentrations, at least with regard to CFC-12.

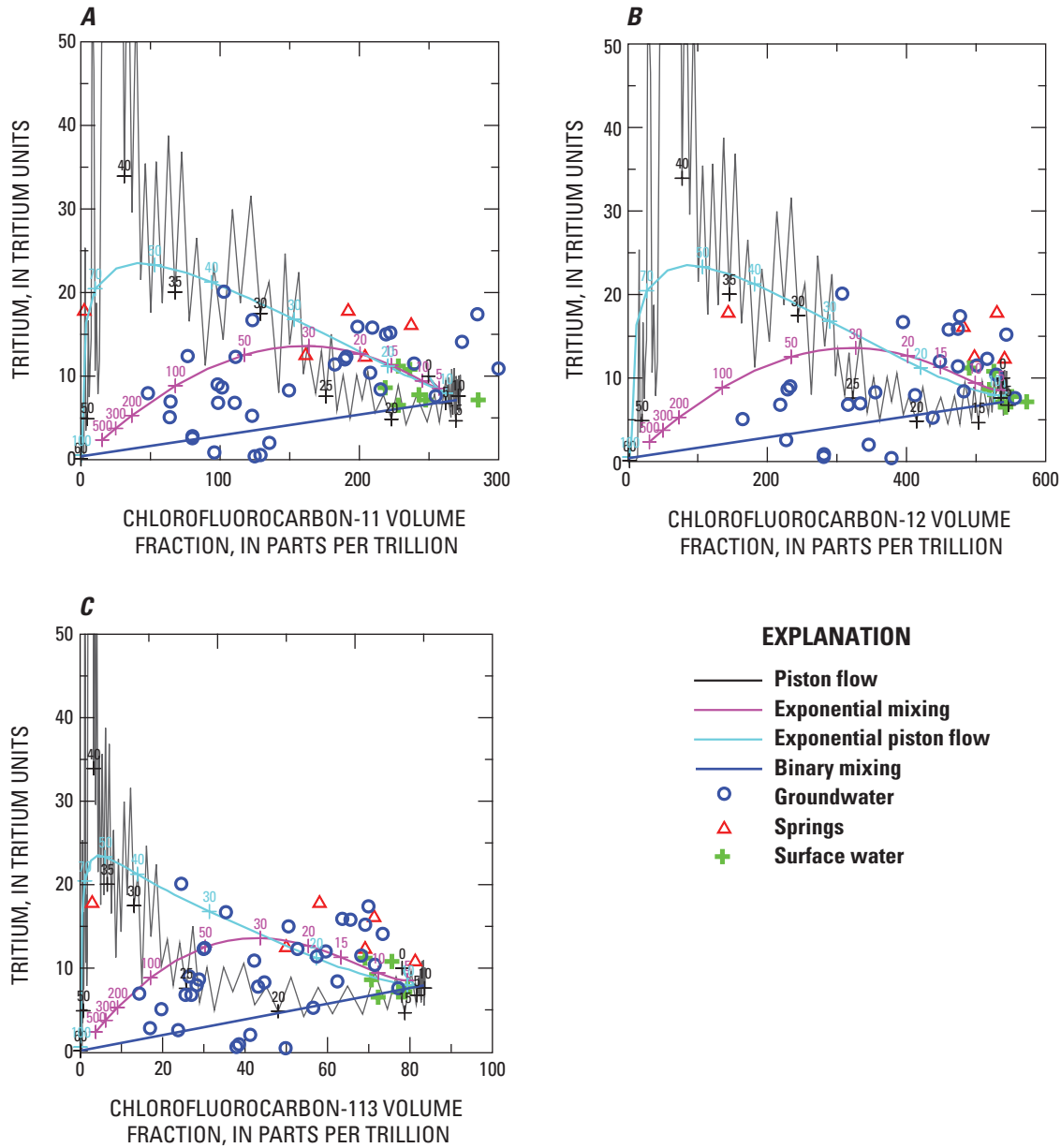


Figure 13-7. Tracer-Tracer plots comparing tritium and CFC volume fractions in groundwater, water from springs, and surface water in the Kabul Basin. The black line represents piston flow, corresponding to CFC volume fractions in parts per trillion (ppt) in North American air and tritium in Kabul Basin precipitation decayed to the sampling year 2006. The blue line represents binary mixing of modern water and old, tracer-free water. Model results for the exponential mixing model (magenta) and exponential-piston model (cyan) also are shown (A) Tritium versus CFC-11; (B) Tritium versus CFC-12; and (C) Tritium versus CFC-113. Selected mean ages in years are given at plus signs along the piston-flow, exponential mixing and exponential-piston-flow lines.

References Cited

- Cook, P.G., and Böhlke, J.K., 1999, Determining time scales for groundwater flow and solute transport using environmental tracers, *in* Cook, P.G., and Herczeg, A., eds., *Environmental Tracers in Subsurface Hydrology*: Boston, Mass., Kluwer Academic Publishers, p. 1–30.
- Eriksson, E., 1958, The possible use of tritium for estimating groundwater storage: *Tellus*, v. 10, p. 472–478.
- International Atomic Energy Agency (IAEA)/WMO, 2004, Global network of isotopes in precipitation: The GNIP database, accessible at <http://isohis.iaea.org>.
- International Atomic Energy Agency (IAEA), 2006, Use of chlorofluorocarbons in hydrology: A guidebook: STI/PUB/1238, 277 p., 111 figs., online at ISBN 92-0-100805-8, http://www-pub.iaea.org/MTCD/publications/PDF/Pub1238_web.pdf
- Małozzewski, P., and Zuber, A., 1982, Determining the turnover time of groundwater systems with the aid of environmental tracers, 1. Models and their applicability: *Journal of Hydrology*, v. 57, p. 207–231.
- Małozzewski, P., Rauert, W., Stichler, W., and Herrmann, A., 1983, Application of flow models to an Alpine catchment area using tritium and deuterium data: *Journal of Hydrology*, v. 66, p. 319–330.
- Michel, R.L., 1992, Residence times in river basins as determined by analysis of long-term tritium records: *Journal of Hydrology*, v. 130, nos. 1–4, p. 367–378.
- Plummer, L.N., Bohkle, J.K., and Busenberg, Eurybiades, 2003, Approaches for groundwater dating, *in* Lindsey, B.D., Phillips, S.W., Donnelly, C.A., Speiran, G.K., Plummer, L.N., Bohlke, J.K., Focazio, M.J., Burton, W.C., and Busenberg, Eurybiades, eds., *Residence times and nitrate transport in groundwater discharging to streams in the Chesapeake Bay Watershed*: U.S. Geological Survey Water-Resources Investigations Report 03–4035, p. 12–24.
- Vogel, J.C., 1967, Investigation of groundwater flow with radiocarbon: *Isotopes in Hydrology*, IAEA, Vienna, p. 355–369.

This page intentionally left blank.

Appendix 14. Simulation of the Groundwater-Flow System

Contents

Simulation of the ground-water flow system	232
Model limitations.....	232
Direct recharge and evaporation.....	234
Stream inflows, leakage, and outflows	234
Hillside groundwater inflows	234
Domestic water use.....	235
Agricultural water use	235
Neogene aquifer	236
Model calibration and parameter sensitivity	236
References cited.....	239

Figures

Figure 14-1. Observed and simulated groundwater levels in the Kabul Basin, Afghanistan	238
--	-----

Tables

Table 14-1. Model parameters and sensitivity in the conceptual groundwater flow system for the Kabul Basin, Afghanistan.	233
---	-----

Appendix 14. Simulation of the Groundwater-Flow System

The various components of the groundwater flow system were estimated on the basis of results of this study, information obtained from other investigations, and groundwater-flow simulations. Mean monthly fluxes, inflows and outflows, in the Kabul Basin aquifer system are presented in table 8. The hydrologic components of the Kabul Basin were summarized by northern subbasins and southern subbasins that can be considered hydrologically separate sub-regional flow systems. The fluxes were estimated on the basis of calculated base flows into and out of the Kabul Basin, actual evapotranspiration (AET), chemical and isotopic information, and knowledge of the basin hydrology gained in this investigation. The mean monthly fluxes were estimated using information from different periods of time (historical and recent). The differences between mean inflows and outflows presented in table 8 were not balanced on an annual basis and, at the monthly scale, the differences include errors from multiple or undifferentiated components of the flow system. Changes in groundwater storage may account for a large portion of the monthly difference in fluxes in nongrowing seasons and an undefined portion of the differences during the growing season. It is not known to what magnitude of estimated recharge, evapotranspiration (considered as a component of net recharge), irrigation leakage, or a combination of these and other factors were represented in the monthly differences during the growing season. The fluxes are therefore considered general approximations of the components of the regional groundwater flow system. Because of the uncertainties in the flux estimations, and numerical simulation of the various components of the flow system discussed in the following sections, the groundwater-flow simulation used mean annual inflow rates with a steady-state model. Because of the limitations of using historical streamflow data with recent water-level data, and the unknown magnitude of irrigation leakages, no attempt was made to simulate transient monthly fluxes as represented in table 8.

Model Limitations

The groundwater-flow model of the Kabul Basin provides a regional-scale simulation of groundwater flow and water balance but is not intended for site-specific analysis. Ground-water-flow models are a numerical representation of the physical flow system and require simplifications and assumptions. Limitations are inherent in the practical application of ground-water-flow models, and the assumptions and simplifications incorporated in a model depend on the intended use of that model. For example, the Kabul Basin model does not simulate unsaturated-zone flow processes (groundwater flow above the water table), or the direct, or overland, component of streamflow; instead, the model simulates the base-flow component of streamflow, or ground-water discharge. Evapotranspiration also is not specifically simulated but is accounted for within a net (or effective) recharge. Other model simplifications include the parameterization of hydrogeologic properties and characteristics into homogenous units and the assignment of these parameters to groups of cells with areas of 400 m by 400 m and thicknesses that depend on the model layer. Simplification also includes the temporal grouping of recharge, streamflow, and groundwater-flow characteristics into a median annual period.

Some components of the flow system could only be approximated given the limitations of this investigation, for example, the groundwater inflows at the mountain front as represented by general-head boundaries (GBH). Although final model parameter values and sensitivities are presented in table 14-1 the simulation model is not considered to be fully calibrated because of the limited input data. Some of these limitations are reflected by large 95-percent confidence intervals for some parameters (table 14-1). However, the simulation supports the conceptual understanding of the groundwater-flow system. The simulation results can be considered to provide a general representation of probable groundwater-flow conditions but are not intended for use at the local scale.

Table 14-1. Model parameters and sensitivity in the conceptual groundwater flow system for the Kabul Basin, Afghanistan.

[E, exponential; C.I., confidence interval, m/d, meters per day; n.a., dimensionless factor; -, CI is not meaningful or is more than 5 orders of magnitude from the parameter value]

Parameter name	Sensitivity (dimensionless)	Sensitivity rank	Upper 95 percent C.I.	Final value	Lower 95 percent C.I.	Units	Parameter description, recharge zone, or hydrogeologic material group
Rech1	2.4E-01	14	7.E-02	1.E-03	2.E-05	m/d	Infiltration recharge rate, Panjsher subbasin
Rech2	7.1E-01	9	9.E-02	1.E-03	2.E-05	m/d	Infiltration recharge rate, western Shomali subbasin
Rech3	1.2E-01	16	1.E+00	1.E-03	1.E-06	m/d	Infiltration recharge rate, southern Central Kabul and Logar subbasins
Rech4	6.8E+00	2	1.E-03	7.E-04	3.E-04	m/d	Areal recharge rate, entire Kabul Basin
STR1	7.1E+00	1	5.E+00	3.E+00	2.E+00	n.a.	Streambed hydraulic conductance factor,
K1	6.6E-01	10	7.E+02	5.E+01	4.E+00	m/d	Horizontal hydraulic conductivity, fan alluvium and colluvium
K1v	7.2E-04	23	-	5.E+00	0.E+00	m/d	Vertical hydraulic conductivity, fan alluvium and colluvium
K2	7.6E-02	18	5.E+06	1.E+02	2.E-03	m/d	Horizontal hydraulic conductivity, river channel sediments
K2v	1.5E-04	24	-	1.E+01	-	m/d	Vertical hydraulic conductivity, river channel sediments
K3	4.5E+00	3	9.E+01	2.E+01	4.E+00	m/d	Horizontal hydraulic conductivity, loess
K3v	8.7E-03	21	-	2.E+00	-	m/d	Vertical hydraulic conductivity, loess
K4	3.0E-01	13	7.E+02	2.E+00	6.E-03	m/d	Horizontal hydraulic conductivity, conglomerates and sandstone
K4v	2.4E-02	20	-	2.E-01	-	m/d	Vertical hydraulic conductivity, conglomerates and sandstone
K5	2.1E+00	5	2.E+02	2.E+00	2.E-02	m/d	Horizontal hydraulic conductivity, upper Neogene
K5v	7.5E-01	8	-	2.E-01	-	m/d	Vertical hydraulic conductivity, upper Neogene
K6	1.8E+00	6	1.E+02	5.E+00	2.E-01	m/d	Horizontal hydraulic conductivity, lower Neogene
K6v	8.8E-02	17	-	5.E-01	-	m/d	Vertical hydraulic conductivity, lower Neogene
K7	1.5E-01	15	-	1.E-01	-	m/d	Horizontal hydraulic conductivity, sedimentary rocks
K7v	8.3E-04	22	-	1.E-01	-	m/d	Vertical hydraulic conductivity, sedimentary rocks
K8	3.6E+00	4	3.E-02	1.E-02	4.E-03	m/d	Horizontal hydraulic conductivity, metamorphic and igneous rocks
K8v	5.1E-01	11	1.E+00	1.E-02	8.E-05	m/d	Vertical hydraulic conductivity, metamorphic and igneous rocks
GHB1	3.5E-01	12	5.E+03	1.E-02	-	n.a.	General-head boundary hydraulic conductance, Paghman Mountains
GHB2	4.0E-02	19	-	1.E-02	-	n.a.	General-head boundary hydraulic conductance, southern mountains
GHB3	1.6E+00	7	2.E+01	1.E-01	4.E-04	n.a.	General-head boundary hydraulic conductance, Kofi Safi Mountains

Direct Recharge and Evaporation

Average annual precipitation is low in the Kabul Valley; between 1959 and 1971 it was 329 mm/yr (Böckh, 1971). Evaporation rates are high, approximately 1,600 mm/yr, relative to annual total precipitation; therefore, direct groundwater recharge by precipitation in the Kabul Valley is generally near zero on an annual basis. Houben and Tunnermeier (2005) estimated annual recharge to be zero for a few years during the early 2000s. Mean monthly precipitation (table 1) historically was highest between February and April (58 to 84 mm), moderate in the late fall and winter months (November to January, 21 to 33 mm), and very low in the summer months (June to October, 1 to 5 mm). Regional evaporation has been calculated to range from 140 to 220 mm/mo during the growing season (April to September). Therefore, recharge by direct infiltration of precipitation generally occurs only from late fall to early spring. Recharge was applied on a regional aerial basis in the conceptual model using the Recharge package (Harbaugh and others, 2000) where a net recharge is applied consisting of the monthly mean rate of precipitation minus the evaporation rate. Where the valley floor is covered by loess (fig. 2), because of the clay content of the loess (appendix 7), infiltration rates in the loess can be expected to be lower and evaporation rates higher than the quaternary sediments. A BGR investigation in Kabul (Niard, 2007) calculated a maximum potential infiltration rate of 39.1 mm/m² for sandy soils and 20.5 mm/m² (or 75 percent of maximum rates) for direct precipitation on loess; therefore, simulated recharge was reduced by 75 percent in loess-covered areas.

Monthly recharge by direct infiltration of precipitation was assumed to be zero for the months where precipitation was low and evaporation was high, June through October. For December through April, the monthly direct recharge rate varies and was estimated to range up to about 3⁻³ m/d during spring runoff (table 14-1). During the nongrowing season, recharge by direct infiltration of precipitation on the aquifers in the subbasins, on the basis of precipitation and evaporation (Böckh, 1971; Houben and Tunnermeier, 2005), may be approximately 30 mm/yr. A mean annual net (recharge minus ET) direct recharge rate was estimated by analysis of base flows and conceptual groundwater-flow simulation to be approximately 0.7⁻³ m/d. Recharge was further distributed to simulate irrigation leakage; in agricultural areas, a recharge rate about two times the areal rate was applied.

Stream Inflows, Leakage, and Outflows

Leakage from the major rivers flowing through the basin has been identified as a source of recharge to the Kabul Valley (Böckh, 1971). The major river channels are generally comprised of coarse-grained sands and gravels (fig. 2) and incise the fine-grained surficial sediments (loess) where present. The river channels represent areas with considerable

potential for infiltration (Niard, 2007). Rivers and streams in the Kabul Basin were simulated with the MODFLOW Stream package (Prudic and others, 2004) in the model layer 1 subbasin areas (figs. 1 and 8). Inflows were simulated at four rivers that flow into the northern subbasins and four rivers that flow into the southern subbasins (figs. 1 and 4). Outflows at the Panjsher River at Shukhi, for the northern subbasins, and the Kabul River at Tang-i-Gharu, for the southern subbasins, capture all streamflow out of the Kabul Basin. The groundwater flow model does not simulate streamflow, but rather the component of streamflow comprised of groundwater discharge. Therefore, a mean monthly base-flow rate calculated using streamflow partitioning methods (Rutledge, 1998) was used to represent river inflows to the model area (table 14-1). Base flows are generally slightly less than mean streamflows for a similar period. Use of base flows in the groundwater flow model reflects the fact that during periods of high flows only a relatively small fraction of the streamflow might infiltrate to the aquifer system.

The perennial streams that flow into the basin from upland areas (fig. 4) contribute inflows to the model and were simulated with the Stream package in model layer 1 in subbasin areas (figs. 1 and 8). Streams were not simulated in the upland areas of the model represented by model layer 2. Inflows from upland areas of the Paghman Mountains were calculated assuming that inflows occur at a rate equal to that of similar upland drainages elsewhere in the study area, and were simulated where tributary streams cross into model layer 1. Mean annual base flow (0.017 m³/s/km²) calculated at the Shatul River drainage, a 202-km² area with no glaciers, was believed to be representative of upland discharges adjacent to the study area and was used to approximate inflows at perennial upland tributaries to the Barik Ab stream, at the Western Front Source Area (fig. 1), and the Paghman and Upper Kabul Rivers, representing areas of about 321 km² and 95 km², respectively. Streams on the east side of the Kabul Basin (Deh Sabz subbasin) are ephemeral and were simulated without a specified headwater inflow.

Streamflow losses at measured at gaged sections of several rivers in the Kabul Valley are presented by Böckh (1971) and indicate very permeable streambeds with the potential for high rates of leakage. Although streambed hydraulic conductivity is probably on the order of 10s of meters per day, streambed hydraulic conductivity was simulated at 2 m/d to prevent numerical oscillation. Streams were simulated with a riverbed width of 10 m for larger rivers to 1 m for smaller streams. Stream stage was assumed to be 1 m below the DEM surface with a 1 m thick riverbed.

Hillside Groundwater Inflows

Monthly mean base flows discussed above can be considered to be primarily composed of groundwater discharge with the exception of snowmelt periods. The base flows to perennial streams, because they are not in glacially

covered areas, represent groundwater discharge that was channeled in the upland drainage area and expressed as streamflow. Precipitation on the hillsides or mountains also seeps through the hillsides or mountains and enters the subbasin valley aquifers laterally as groundwater flow at the valley walls. Isotopic sampling indicates that this is likely a source of recharge to the Western Front Source Area and Eastern Front Source Area (fig. 1). Where high-elevation upland areas are adjacent to the subbasins, groundwater inflows are likely to occur. The presence of winter snowpack would likely contribute to recharge to the hillside bedrock aquifers that may provide delayed groundwater inflows to the subbasins during periods with less recharge.

The drainage divide at the eastern flank of the Kabul Basin is immediately adjacent to the Deh Sabz subbasins and very little upland area slopes towards the basin from the east. However, some groundwater likely flows into the Deh Sabz from the drainage area east of the Deh Sabz. Support for this include perennial springs that originate at the base of the hillside (Akbari and others, 2007); isotopic sample results indicate that the groundwater at the Eastern Front Source Area is distinguishable from groundwater in the other areas of the Deh Sabz subbasin; and heads at wells 4, 7, and 59.1 (Akbari and others, 2007) are approximately 100 to 200 m greater than the elevation of the nearest perennial river, the Kabul River. The mountain ridge east of Deh Sabz is composed of sandstones and limestones (Bohannon and Turner, 2007) and is likely to have a greater porosity and water storage and transmitting capacity than bedrock elsewhere in the study area. For example, isotopic analysis (fig. 25) indicates a regional age and depth relation to groundwater that results from a combination of direct precipitation recharge and irrigation leakage. An outlier on figure 25 from a sample collected from the eastern area of the Deh Sabz subbasin does not fit the regional trend in that the groundwater is much younger than expected at depth. This well is in an area where no irrigation is present and likely receives the least amount of precipitation recharge in the Kabul Basin. This sample indicates that hillside groundwater inflows occur at the Eastern Front Source Area adjacent to the Kohe Safi Mountains.

Groundwater inflows were simulated in model layer 2 (fig. 8) using the MODFLOW-2000 general-head boundary (GHB) package (Harbaugh and others, 2000) at the base of hillsides that form the perimeters of Kabul Basin (equivalent to the lateral extent of model layer 1). Heads in the Quaternary aquifer at the base of such hillsides varied from 10 to about 50 m below the land surface. A head equal to the midpoint of model layer 1 thickness was used in the general-head boundary. The hydraulic conductance, a dimensionless multiplication factor used in the GHB package, was 0.01 at igneous and metamorphic hillsides such as the Paghman Mountains and 0.1 at sedimentary rocks such as the Kohe Safi Mountains. Without additional inflows, particularly at the Eastern Front Source Area of the Deh Sabz subbasin,

simulated groundwater levels were generally too low at the valley walls. However, this inflow represents a small fraction (about one tenth) of the total simulated flux in the Kabul Basin.

Domestic Water Use

Groundwater withdrawals for domestic purposes were approximated by applying a per-capita water-use rate times the estimated population by kilometer-scale geographic information system (GIS) grid cells (fig. 26). Withdrawals were simulated in model layer 1, using the WEL package (Harbaugh and others, 2000), at grid cells with a population greater than 10. A per-capita water-use rate of 30 L/d was used in urban areas. A lower per-capita rate was initially considered for rural areas; however, rural water use likely includes additional water uses for gardens and livestock and may be comparable to urban-use rates. A per-capita water-use rate of 20 L/d was used in rural areas.

Future water uses were simulated by increasing the simulated current water use by a factor of six following present population patterns (fig. 26). Future water uses were also examined by simulating withdrawals in the lower Neogene aquifer at major population centers to represent hypothetical municipal supply centers.

Agricultural Water Use

Agriculture in the Kabul Valley relies primarily on irrigation and less so on rainfall early in the growing season of April through September. Irrigation water is generally obtained from nearby streams and, to a lesser degree, is also supplied by karezes, springs, and wells. There are no records of the amount of water used in the Kabul Basin or how it is distributed; however, the efficiency of water applied on crops has been reported to be about 25 to 30 percent because of leakage and evaporation (Banks and Soldal, 2002). As discussed previously, agricultural water use can be inferred from analysis of land cover in satellite imagery. Larger croplands represent areas where streamflow has been diverted for irrigation and may also infiltrate to the subsurface. Senay and others (2007) estimated rates of actual ET for the three main agricultural areas in the Kabul Basin that are termed in this report: (1) the *northern area*, in the Panjshir River and Bagram area; (2) the *western area*, at the flank of the Paghman Mountains in the flood plain of the Barik Ab River, south of the confluence with the Panjshir River; and (3) the *southern area* in the flood plain of the Paghman, Kabul, and Logar Rivers.

The majority of the irrigated water is from streamflow diversion to irrigation canals during periods of available streamflow. Later in the summer months, particularly August and September, little or no flow is available for irrigation in the rivers in the southern half of the study area (figs. 13 and

14) including the perennial streams originating in the Paghman Mountains. Pumped groundwater is not likely to be a large contribution to the total irrigation because of the expense of fuel and the infrastructure needed to supply large amounts of water. Where present, karezes and springs provide water for irrigation; however, these sources are also likely to contribute a lesser amount of water because springs and karezes are not numerous and groundwater declines in recent years may have reduced their productivity (Banks and Soldal, 2002). During the summer months, the rivers in the Kabul area are generally depleted by intense irrigation (Böckh, 1971).

The water used for agriculture is diverted from streams flowing into, or through, the Kabul Basin and the transpiration component (AET, fig. 7) represents a loss of water from the system. Because irrigation efficiencies are expected to be large (50 percent or more), the irrigation areas and the AET water-use rates provide locations and relative magnitudes where recharge occurs, in the form of irrigation leakage, to the groundwater system. The magnitude of irrigation-derived recharge is not known and could not be differentiated from areal recharge, for simulation in the groundwater flow model, with the information available. Recharge due to irrigation leakage is likely equal to or greater than areal recharge and was simulated at a mean annual rate of 1.2^{-3} m/d, or nearly twice the areal recharge rate (0.7^{-3} m/d).

Neogene Aquifer

The expected growth in Kabul will require additional water for domestic and agricultural uses. A potential source of future water supply for Kabul may be the Neogene aquifer, which underlies the Pleistocene and recent aquifers that are presently in use (fig. 8). The hydraulic characteristics and quality of water in the Neogene aquifer are not well known because of the difficulties and expense of drilling deep wells in Kabul. However the Soviet "Passport" investigations of the late 1970s (Japan International Corporation Agency, 2007b) and recent Japan International Corporation Agency (2007a, b) investigations indicate that the thickness of the aquifer is more than 600 m in some subbasins, which may provide considerable storage. The Neogene generally consists of fine-grained, compact sediments with corresponding low permeabilities and is differentiated by Japan International Corporation Agency (2007b) into an upper and lower aquifer. The upper Neogene aquifer extends to about 400 to 500 m below land surface and consists of a mudstone, a clay, and clay with gravel. The lower Neogene may extend up to 1,000 m or greater (Homilius, 1969), in some localized areas near the centers of some subbasins, and consists of gravel and sand with mudstone. However, borehole geophysical logs contained in Passport reports and recently collected by Japan International Corporation Agency (2007b) indicate that a coarse-grained basal conglomerate is present in some locations in the lower Neogene formation. Such coarse-grained lenses may not be laterally continuous; however,

discontinuous lenses may permit water to be extracted from the surrounding low permeability aquifer. The sustainability of large withdrawals from the Neogene aquifer are not known but can be assessed with hypothetical simulations.

To assess the source of water to the Neogene aquifer and assess the potential impact of large withdrawals on the water resources of Kabul, several hypothetical supply wells were simulated at major population centers in the subbasins. This analysis does not assess the likelihood of suitable locations for withdrawals in the Neogene aquifer or the quality of water withdrawn. The withdrawals were assessed with respect to impact on water levels in the overlying aquifer, which would affect existing water uses, and the source of water withdrawn, which would indicate the potential sustainability of the withdrawal. The simulated well does not imply that the location is a favorable location for groundwater extraction. The implications of the impact of multiple withdrawals in each basin can be qualitatively inferred from the results presented. Withdrawal wells were simulated in the upper 100 m of model layer 3 to represent withdrawals from the upper Neogene aquifer.

Withdrawals in the Neogene aquifer near the flank of the Paghman Mountains may be more successful than withdrawals from other areas of the Kabul Basin because of recharge from the upland areas and increased storage in the underlying bedrock. The bedrock in this area is likely to be more highly fractured than elsewhere in the study area because of a greater density of faults in this area (Ruleman and others, 2007). Water stored in the underlying bedrock aquifer also may be recharged from precipitation on the mountains through fracture zones. However, withdrawals in this area may reduce flows to streams or karezes in the area. Withdrawals in the Dez Sabz subbasin, and near the eastern mountain flanks in the Shomali Plain, may be sustainable depending on groundwater inflows from the Kohe Safi Mountains.

Model Calibration and Parameter Sensitivity

The steady-state model was calibrated to observations of groundwater and surface-water levels and groundwater discharge to streams following the methods of Hill (1998) and Hill and others (2000). The model was calibrated in a regional manner, where model characteristics were adjusted by parameter zones, which form relatively large geologic or hydrologically consistent areas. For example, the hydraulic conductivity of each geologic unit was kept consistent within that unit and changes were made to the unit as a whole. Geohydrologic units used were eight broad classifications consisting of four unconsolidated sediment units (Quaternary sediments, loess, river-channel sediments, and upper and lower Neogene sediments), and two general bedrock units; metamorphic and igneous, as one unit, and sedimentary rock as a second unit (appendix 6). Parameters used in the model include the hydraulic characteristics used to define the geohydrologic units and other features such as recharge

or streambed conductivity. Although a better model fit between observed and simulated data could likely be obtained by locally adjusting cells within parameter zones, such modifications made without a conceptual basis do not improve the understanding of hydrologic processes and may not result in a realistic model. Instead, the goal of the calibration process is to help understand regional hydrogeologic processes as opposed to matching observations. In the parameter estimation process used in this study, not all parameters were estimated in one simulation. Selected parameters were estimated while some were held fixed. The procedure was repeated, with other parameters estimated or held fixed, until optimal parameter values, with reasonable values, were identified for all parameters. The sensitivity of the parameters was evaluated simultaneously with optimized values (table 14-1).

Model calibration is dependant on observations of the groundwater flow system. Because the observations of streamflows relied on historical data, a quantitative analysis of model calibration was not realistic. However, the general nature of streamflows into and out of the Kabul Basin are known and groundwater-level data were available (Akbari and others, 2007), which allow for an approximate calibration (fig. 14-1) and analysis of model parameter sensitivity (table 14-1). Observations are used to find the best-fit model parameters, and the known or estimated error of the observations are used to calculate the sensitivity of the groundwater flow model to the model parameters. Observations include measured or estimated groundwater heads and groundwater discharges (base flows). Age of groundwater samples was used qualitatively as an observation. Although observation error is rarely known in practice, it can be estimated and parameter values are generally not very sensitive to moderate changes in the weights used (Hill, 1998). By this process, data sets with greater accuracy are given greater weight in the parameter-estimation process; this permits data sets with different levels of accuracy to be used simultaneously in the parameter-estimation process. The steady-state parameter sensitivity was calculated with all model layers simulated as non-convertible (saturated) layers to "linearize" the numerical calculations. Although in the natural system some areas are likely to become unsaturated, simulating all layers in the numerical model as saturated (non-convertible), greatly simplifies the numerical calculations allowing for solution of the parameter sensitivities. The simplification (linearization) approach used in this study is presented as a guideline for effective model calibration described by Hill (1998). Groundwater-flow simulations used to assess water availability in the Kabul Basin were conducted with model layer 1 unconfined (convertible).

Approximate weights were assigned to observation groups to represent data with differing accuracies. Groundwater levels (heads) used in model calibration were obtained from three sources to provide aerially distributed calibration points: (1) observations collected by Danish Committee for Aid to Afghan Refugees (DACARR) during recent (post-2000) shallow-well installations (Safi and

Vijsselaar, 2007); (2) a historical well database containing water levels collected during installation of supply wells primarily in the 1970s and 1980s, also maintained by DACAAR (Eng. Hassan Saffi, DACAAR, written commun., 2007); and (3) and water levels monitored by Afghanistan Geological Survey (AGS) (Akbari and others, 2007). Groundwater elevations derived from the first two data sets were calculated by subtracting depth to water from the measurement point, which in this case was the model cell surface elevation (interpreted from the DEM). The first data set was considered to be accurately located, the second data set was approximately located from street addresses, and the third data set was accurately located (Akbari and others, 2007). The measurement-point elevation is the primary source of water-level error in this data set; therefore, the completion report water-level data are weighted on the basis of measurement-point accuracy. Given the uncertainties involved in well location and measurement, a standard deviation of 10 m was used for water-level observations from the first 2 data sets, and 1-m for the third.

The Kabul Basin groundwater balance was simulated using the mean annual base flow (table 8) as inflows to the rivers entering the basin (fig. 4). Simulated base flows out of the basin were calculated at the Panjsher (2,260,000 m³/d) and Kabul Rivers (550,000 m³/d), at the model boundary (fig. 4), and were comparable to median annual outflows (2,984,000 and 856,000 m³/d, respectively) in table 8. The model more closely represents median flow conditions and the median flows are probably a better indicator of long-term groundwater-flow conditions than mean flows. The hydraulic properties for sediments and rocks, described in appendix 6, and the rate of recharge and irrigation leakage were adjusted, in a parameter estimation and user guided iterative process, to calibrate the conceptual model to mean flows and heads. Regionally simulated hydraulic properties and the sensitivity of the simulated groundwater flow to selected model parameters are provided in table 14-1.

Simulated groundwater levels compared favorably to historical groundwater-level observations by subbasin (fig. 14-1). Simulated groundwater levels in the valley bottoms, or subbasin centers, were generally within 10 m of historic or recent mean values. However, larger errors were apparent near the valley walls where some heads were much lower than the observations. This illustrates a common difficulty of representing a valley-aquifer system, with considerable relief, with a numerical groundwater-flow model. Errors in simulated heads at the valley walls indicate also that the conceptualization of the groundwater flow system, at this location in the model, and the magnitude and distribution of groundwater inflows from the adjacent bedrock hillsides, is not well known. The conceptual model parameters with the greatest sensitivity include (table 14-1): streambed conductance, areal recharge, K3 (loess horizontal hydraulic conductivity), K8 (sedimentary rock horizontal hydraulic conductivity), K5 (upper Neogene horizontal hydraulic conductivity), K6 (lower Neogene

horizontal hydraulic conductivity), and GBH (general head boundary). The conceptual model was least sensitive to model parameters representing vertical conductivities. This can be expected given that there are few stresses with depth and no measurements of vertical head gradients. A number of parameters have an upper and (or) lower 95-percent

confidence interval more than a few orders of magnitude from the parameter value (table 14-1). This reflects the fact that there are few or no observation data with which to qualify or constrain some parameters.

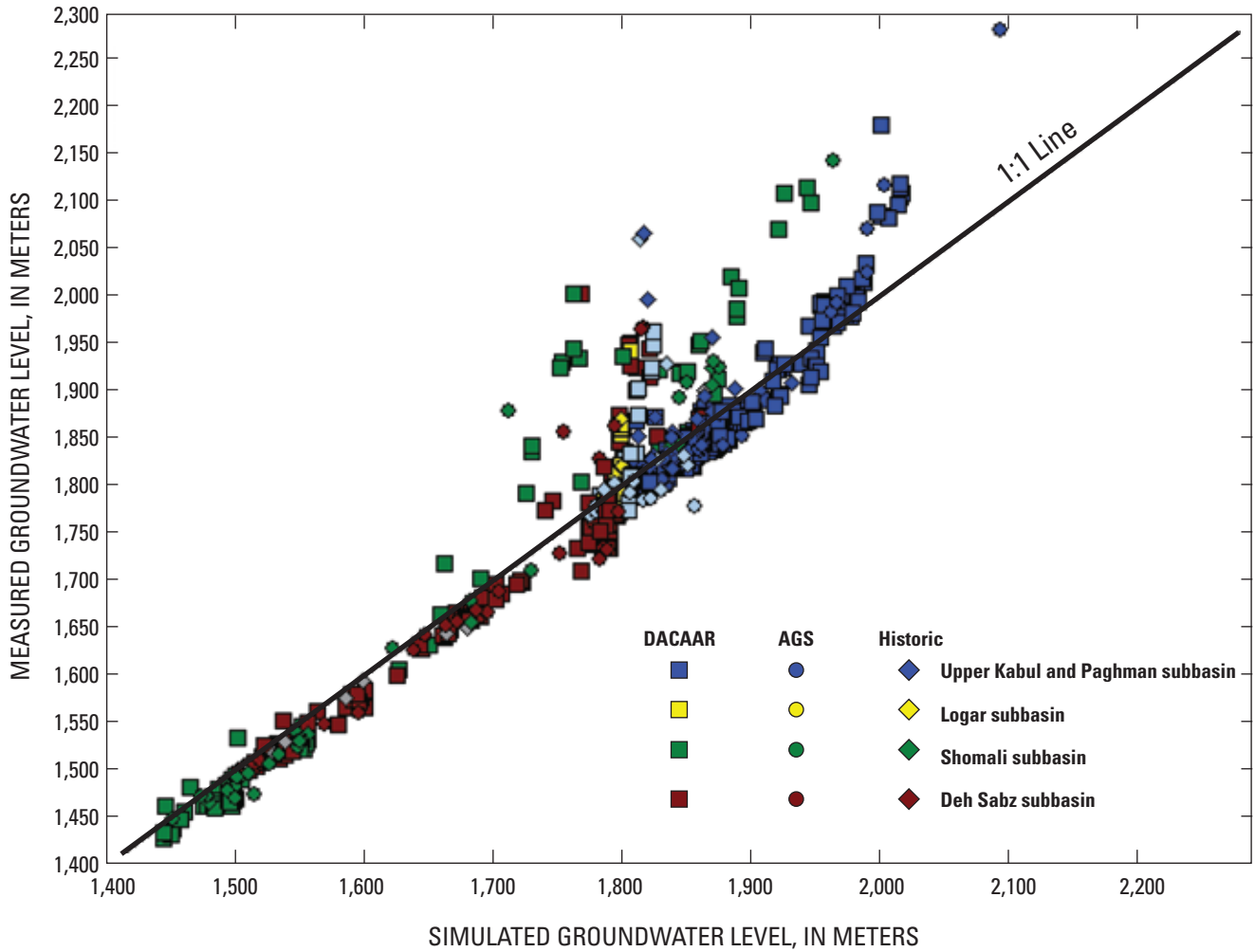


Figure 14-1. Observed and simulated groundwater levels in the Kabul Basin, Afghanistan. Data points include water levels measured by the Danish Committee for Aid to Afghan Refugees (DACAAR), the Afghanistan Geological Survey (AGS), and at water-supply wells installed before 1980 (Historic)

References Cited

- Akbari, M.A., Tahir, M., Litke, D.W., and Chornack, M.P., 2007, Groundwater levels in the Kabul Basin, Afghanistan, 2004–07: U.S. Geological Survey Open-File Report 2007–1294, 46 p.
- Banks, David, and Soldal, Oddmund, 2002, Towards a policy for sustainable use of groundwater by non-governmental organizations in Afghanistan: *Hydrogeology Journal*, v. 10, p. 377–392.
- Böckh, E.G., 1971, Report on the groundwater resources of the city of Kabul, report for Bundesanstalt für Geowissenschaften und Rohstoffe [unpublished]: BGR file number 0021016, 43 p.
- Bohannon, R.G., and Turner, K.J., 2007, Geologic map of quadrangle 3468, Chak Wardak-Syahgerd (509) and Kabul (510) quadrangles, Afghanistan: U.S. Geological Survey Open-File Report 2005–1107–A. 1 sheet.
- Harbaugh, A.W., Banta, E.R., Hill, M.C., and McDonald, M.G., 2000, MODFLOW-2000, the U.S. Geological Survey modular groundwater-flow model—User guide to modularization concepts and the groundwater flow process: U.S. Geological Survey Open-File Report 00–92, 121 p.
- Hill, M.C., 1998, Methods and guidelines for effective model calibration: U.S. Geological Survey Water-Resources Investigations Report 98–4005, 90 p.
- Hill, M.C., Banta, E.R., Harbaugh, A.W., and Anderman, E.R., 2000, MODFLOW-2000, the U.S. Geological Survey modular groundwater model—User guide to the observation, sensitivity, and parameter-estimation process and three post-processing programs: U.S. Geological Survey Open-File Report 00–184, p. 209.
- Homilius, Joachim, 1969, Geoelectrical investigations in east Afghanistan, *Geophysical Prospecting*, v. 17, issue 4, p. 468–487.
- Houben, Georg, and Tunnermeier, Torge, 2005, Hydrogeology of the Kabul Basin, Part I—Geology, aquifer characteristics, climate and hydrology: Federal Institute for Geosciences and Natural Resources (BGR), Hannover, Germany, p. 45.
- Japan International Cooperation Agency (JICA), 2007a, The study on groundwater resources potential in Kabul Basin, in the Islamic Republic of Afghanistan: 3rd Joint Technical Committee, Sanyu Consultants, Inc., Kabul, Afghanistan, p. 20.
- Japan International Cooperation Agency (JICA), 2007b, The study on groundwater resources potential in Kabul Basin, in the Islamic Republic of Afghanistan: 4th Joint Technical Committee, Sanyu Consultants, Inc., Kabul, Afghanistan, p. 12.
- Niard, Nadege, 2007, Hydrogeology of the Kabul Basin, Part III—Modeling approach, Conceptual and numerical models: Federal Institute for Geosciences and Natural Resources (BGR), Hannover, Germany, p. 103.
- Prudic, D.E., Konikow, L.F., and Banta, E.R., 2004, A new streamflow routing (SFR1) package to simulate stream-aquifer interaction with MODFLOW-2000: U.S. Geological Survey Open-File Report 2004–1042, 95 p.
- Ruleman, C.A., Crone, A.J., Machette, M.N., Haller, K.M., and Rukstales, K.S., 2007, Map and database of probable and possible Quaternary faults in Afghanistan: U.S. Geological Survey Open-File Report 2007–1103, 39 p., 1 pl.
- Rutledge, A.T., 1998, Computer programs for describing the recession of groundwater discharge and for estimating mean groundwater recharge and discharge from streamflow records—Update: U.S. Geological Survey Water-Resources Investigations Report 98–4148, 43 p.
- Safi, Hassan, and Vijselaar, Leendert, 2007, Groundwater monitoring, Evaluation of groundwater data: DACAAR, Kabul, Afghanistan, p. 99.
- Senay, G.B., Buddy, M., Verdin, J.P., and Melesse, A.M., 2007, A coupled remote sensing and simplified surface energy balance approach to estimate actual evapotranspiration from irrigated fields: *Sensors*, v. 7, p. 979–1000.

This page intentionally left blank.